ることができる[15,16].

4．*N*-acety-beta-D-glucosaminidase (NAG)

近位尿細管上皮細胞のリソソーム酵素である．酵素活性の測定が検出法であるため，簡便かつ感度が高い．AKI において損傷を受けた近位尿細管から尿中へ放出され，その尿中の濃度が近位尿細管の損傷の程度ときわめてよく相関する．また，AKI で尿中に放出される酵素の中では，比較的安定である．

5．L-type fatty acid binding protein (L-FABP)

低分子量蛋白質で，さまざまな組織で産生される遊離脂肪酸結合蛋白質である．liver-type (L-type) は近位尿細管で誘導され，脂肪酸代謝におけるキャリアーとして働く．尿中バイオマーカーとして，さまざまな腎疾患でその有用性が研究されている．そのプロモーター領域にストレス応答性の転写因子結合領域を有し，損傷を受けた近位尿細管上皮細胞において発現誘導を受ける．AKI において，尿中へ放出されると思われる．

おわりに

既存の腎機能マーカーを AKI の指標として用いるには限界があり，さらなる迅速性，正確性，および特異性を兼ね備えた新しいバイオマーカーの開発と臨床応用が望まれている．これまで述べてきたように，このような問題点を補完，または克服するための新規 AKI 尿中バイオマーカーの開発，評価が進められている．とくに，ゲノム情報科学を腎臓病学に取り入れることによって，有望な新規尿中バイオマーカーの同定もなされてきた．

血清クレアチニン濃度や BUN に加えて，本文で述べた新規尿中バイオマーカーを併用することによって，バイオマーカーそれぞれの特異性に加え，感度や精度の強化が期待されている．さらに，これらバイオマーカーの新薬開発領域における前臨床試験への応用も，有望視されている．

謝　辞　Drs Bonventre JV, Vaidya VS, Ferguason MA の協力，支援を感謝いたします．

文　献

1) Vaidya VS et al：Biomarkers of acute kidney injury. Annu Rev Pharmacol Toxicol **48**：463, 2008
2) Mehta RL et al：Acute Kidney Injury Network：report of an initiative to improve outcomes in acute kidney injury. Crit Care **11**：R31, 2007
3) Molitoris BA et al：Improving outcomes of acute kidney injury：report of an initiative. Nat Clin Pract Nephrol **3**：439, 2007
4) Bellomo R et al：Acute renal failure-definition, outcome measures, animal models, fluid therapy and information technology needs：the Second International Consensus Conference of the Acute Dialysis Quality Initiative (ADQI) Group. Crit Care **8**：R204, 2004
5) Ichimura T et al：Kidney injury molecule-1 (KIM-1), a putative epithelial cell adhesion molecule containing a novel immunoglobulin domain, is up-regulated in renal cells after injury. J Biol Chem **273**：4135, 1998
6) Ichimura T et al：Kidney injury molecule-1：a tissue and urinary biomarker for nephrotoxicant-induced renal injury. Am J Physiol Renal Physiol **286**：F552, 2004
7) Amin RP et al：Identification of putative gene based markers of renal toxicity. Environ Health Perspect **112**：465, 2004
8) Bonventre JV, Weinberg JM：Recent advances in the pathophysiology of ischemic acute renal failure. J Am Soc Nephrol **14**：2199, 2003
9) Wang H et al：Electrical detection of kidney injury molecule-1 with AlGaN/GaN high electron mobility transistor. Appl Phys Lett **91**：222101, 2007
10) Han WK et al：Kidney injury molecule-1 (KIM-1)：a novel biomarker for human renal proximal tubule injury. Kidney Int **62**：237, 2002
11) Han WK et al：Urinary biomarkers in the early diagnosis of acute kidney injury. Kidney Int **73**：863, 2008
12) Ichimura T et al：Kidney injury molecule-1 is a phosphatidylserine receptor that confers a phagocytic phenotype on epithelial cells. J Clin Invest **118**：1657, 2008
13) Miyanishi M et al：Identification of Tim4 as a phosphatidylserine receptor. Nature **450**：435, 2007
14) Kobayashi N et al：TIM-1 and TIM-4 glycoproteins bind phosphatidylserine and mediate uptake of apoptotic cells. Immunity **27**：927, 2007
15) Mishra J et al：Identification of neutrophil gelatinase-associated lipocalin as a novel early urinary biomarker for ischemic renal injury. J Am Soc Nephrol **14**：2534, 2003
16) Ronco C：N-GAL：diagnosing AKI as soon as possible. Crit Care **11**：173, 2007

Am J Physiol Cell Physiol 295: C632–C641, 2008.
First published July 16, 2008; doi:10.1152/ajpcell.00019.2008.

Identification and functional characterization of a novel human and rat riboflavin transporter, RFT1

Atsushi Yonezawa, Satohiro Masuda, Toshiya Katsura, and Ken-ichi Inui

Department of Pharmacy, Kyoto University Hospital, Faculty of Medicine, Sakyo-ku, Kyoto, Japan

Submitted 11 January 2008; accepted in final form 10 July 2008

Yonezawa A, Masuda S, Katsura T, Inui K. Identification and functional characterization of a novel human and rat riboflavin transporter, RFT1. *Am J Physiol Cell Physiol* 295: C632–C641, 2008. First published July 16, 2008; doi:10.1152/ajpcell.00019.2008.—Absorption of riboflavin is mediated by transporter(s). However, a mammalian riboflavin transporter has yet to be identified. In the present study, the novel human and rat riboflavin transporters hRFT1 and rRFT1 were identified on the basis of our rat kidney mRNA expression database (Horiba N, Masuda S, Takeuchi A, Saito H, Okuda M, Inui K. *Kidney Int* 66: 29–45, 2004). hRFT1 and rRFT1 cDNAs have an open reading frame encoding 448- and 450-amino acid proteins, respectively, that exhibit 81.1% identity and 96.4% similarity to one another. In addition, an inactive splice variant of hRFT1, hRFT1sv, was also cloned. The hRFT1sv cDNA, which encodes a 167-amino acid protein, retains an intron between exons 2 and 3 of hRFT1. Real-time PCR revealed that the sum of hRFT1 and hRFT1sv mRNAs was expressed strongly in the placenta and small intestine and was detected in all tissues examined. In addition, hRFT1 and hRFT1sv were expressed in human embryonic kidney (HEK)-293 and Caco-2 cells. HEK-293 cells transfected with green fluorescent protein-tagged hRFT1 and rRFT1 exhibited a fluorescent signal in the plasma membrane. Overexpression of hRFT1 and rRFT1, but not hRFT1sv, increased the cellular accumulation of [^{3}H]riboflavin. The transfection of small interfering RNA targeting both hRFT1 and hRFT1sv significantly decreased the uptake of [^{3}H]riboflavin by HEK-293 and Caco-2 cells. Riboflavin transport is Na^+, potential, and pH independent. Kinetic analyses demonstrated that the Michaelis-Menten constants for the uptake by HEK-293 and Caco-2 cells were 28.1 and 63.7 nM, respectively. We propose that hRFT1 and rRFT1 are novel mammalian riboflavin transporters, which belong to a new mammalian riboflavin transporter family.

vitamin B2; intestine; absorption; kidney; human embryonic kidney-293 cells

RIBOFLAVIN, A WATER-SOLUBLE vitamin also known as vitamin B2, is essential for normal cellular functions. Its most important biologically active forms, flavin adenine dinucleotide (FAD) and flavin mononucleotide (FMN), act as intermediaries in the transfer of electrons in biological oxidation-reduction reactions. Under conditions of physiological and pathological stress, humans are susceptible to developing riboflavin deficiency. Such a deficiency in pregnancy and adolescence induces developmental abnormalities and has been implicated as a risk factor for anemia, cancer, cardiovascular disease, and neurodegeneration (32).

Humans are unable to synthesize riboflavin and thus acquire it as a nutrient. In vivo, in situ, and membrane vesicle experiments have elucidated the predominant role of carrier-mediated absorption in the intake of riboflavin by the small intestine and colon (4, 7, 17, 21, 24, 34, 41, 44). In addition, the subject of riboflavin excretion has gained increasing attention. Jusko et al. (18, 19) and others (7, 25, 40, 45) demonstrated saturable renal reabsorption and accumulation of riboflavin. Therefore, riboflavin transporters are thought to be essential for the maintenance of riboflavin homeostasis in the intestine and kidney. Since the mid 1990s, the mechanism by which riboflavin is transported has been examined using several human-derived cell lines (14, 15, 20, 23, 36–38). These studies indicated that the cellular uptake of riboflavin was saturable, suggesting that the transporter(s) was (were) intrinsically expressed in these cells. However, a mammalian riboflavin transporter has yet to be identified.

We previously constructed an mRNA expression database by sequencing cDNA clones randomly selected from a rat kidney cDNA library (12). Analysis of the database revealed that 16.7% of its 2,048 genes were of unknown function. As transporter mRNA accounts for 3.7% of the genes of known function in this database, at least 15 novel transporters could be included among the genes of unknown function. We successfully identified a Na^+-dependent D-glucose/D-fructose transporter 1, NaGLT1, which mediates tubular reabsorption of D-glucose and D-fructose (11, 13).

In the present study, we searched for a novel transporter among the functionally unknown genes of this database and identified a human and rat riboflavin transporter (hRFT1 and rRFT1, respectively). An inactive spliced variant of hRFT1, hRFT1sv, was also cloned. The tissue distribution, cellular localization, and functional characterization of these transporters were examined.

MATERIALS AND METHODS

Isolation of rat and human riboflavin transporter 1. We previously constructed a rat kidney mRNA expression database by sequencing cDNA clones randomly selected from a kidney cDNA library (12). Using the SOSUI program (10), we searched among the 2,048 clones of this database for uncharacterized multitransmembrane proteins. One clone encoding a 10-transmembrane protein (GenBank accession no. XM_001075182, similar to G protein-coupled receptor 172B) was identified. On the basis of this sequence, a 5′-rapid amplification of cDNA-ends-polymerase chain reaction (RACE-PCR) and a 3′-RACE-PCR were carried out with the reverse primers 5′-TGGCTCCTGCAATGGTGA-3′ and 5′-TCCTCTGTTCCTGGTGTTTCT-3′, and the forward primers 5′-TTCTTTTGGGTGTTGACGG-3′ and 5′-TTCCAAGGCCTCCTGTTACT-3′ using the rat kidney-derived adaptor-ligated Marathon-Ready cDNA library (Clontech, Palo Alto, CA) according to the manufacturer's instructions. The

Address for reprint requests and other correspondence: K. Inui, Dept. of Pharmacy, Kyoto Univ. Hospital, Sakyo-ku, Kyoto 606-8507, Japan (e-mail: inui@kuhp.kyoto-u.ac.jp).

The costs of publication of this article were defrayed in part by the payment of page charges. The article must therefore be hereby marked "*advertisement*" in accordance with 18 U.S.C. Section 1734 solely to indicate this fact.

RACE fragments were ligated, cloned into the plasmid vector pBK-CMV (Stratagene, La Jolla, CA) or pEGFP-C1 (Clontech), and sequenced using a multicapillary DNA sequencer RISA384 system (Shimadzu, Kyoto, Japan).

In addition, we searched for the human ortholog in the GenBank database by using the TBLASTN algorithm. We identified an ortholog (GenBank accession no. NM_017986.2, G protein-coupled receptor 172B) that exhibited a high degree of similarity to the rat gene. On the basis of the sequence, a 5′- and a 3′-RACE-PCR were performed with the reverse primers 5′-CTCGGTGGCTCCTGCAATGGCAAAG-3′ and 5′-AACAGCAACAGGAGACCCCGGAAGGC-3′, and the forward primers 5′-CCCCTCATACCTCTCTGTGGTTGTGGCG-3′ and 5′-CCCCATCCAGGTGGTACAGGTGCTGAGT-3′ using the human kidney-derived adaptor-ligated Marathon-Ready cDNA library (Clontech). The RACE fragments were ligated and sequenced. We simultaneously obtained an ortholog of rRFT1, hRFT1, and a splice variant hRFT1sv.

A

```
hRFT1      1 MAAPTLGRLVLTHLLVALFGMGSWAAVNGIWVELPVVVKDLPEG-WSLPSYLSVVVALGN  59
hRFT1sv    1 ..............................................E.EGGTGKRGAGMPRK  60
rRFT1      1 ....P.....................I..............E....-.........L.....  59

hRFT1     59 LGLLVVTLWRRLAPGKGEQVPIQVVQVLSVVGTALLAPLWHHVAPVAGQLHSVAFLTLAL  119
hRFT1sv   60 VACGSSLSLSLSHC..DMASFL.CRLEPP.IPLCGCGAGKPGSAGGDPVEAAGPGQGRAGPH  120
rRFT1     59 ....L...........S.RI......G..I...G......SNM.L..............F  119

hRFT1    119 VLAMACCTSNVTFLPFLSHLPPPFLRSFFLGQGLSALLPCVLALVQGVGRLECPPAPTNG  179
hRFT1sv  120 PGGTGAEC.GHSPAGPSVAPRG.SG.AAP.CGLPNSG.GVGNG.LYL-------------  167
rRFT1    119 ...LS..A.....................................A........LHV.A..  179

hRFT1    179 TSGPPL-----DFPERFPASTFFWALTALLVTSAAAFRGLLLLLPSLPSVTTGGSGPELQ  234
hRFT1sv  167 ----------------------------------------------------------  167
rRFT1    179 .T...IKVSPIN.....S.G....V.....G......Q.........P.PEA.M.T.--.R  237

hRFT1    234 LGSPGAEEEEKEEEEALPLQEPPSQAAGTIPGPDPEVHQLFSAHGAFLLGLMAFTSAVTN  294
hRFT1sv  167 ----------------------------------------------------------  167
rRFT1    237 VET..T....-.....S......G.V.SIVSS...KA.R...SRS.C....L.I.N.L..  296

hRFT1    294 GVLPSVQSFSCLPYGRLAYHLAVVLGSAANPLACFLAMGVLCRSLAGLVGLSLLGMLFGA  354
hRFT1sv  167 ----------------------------------------------------------  167
rRFT1    296 ....A.....................S..........A.........Y..C....F..T  356

hRFT1    354 YLMALAILSPCPPLVGTTAGVVLVVLSWVLCLCVFSYVKVAASSLLHGGGRPALLAAGVA  414
hRFT1sv  167 ----------------------------------------------------------  167
rRFT1    356 ...T..V...........S..............AG....I...T..M..S.........  416

hRFT1    414 IQVGSLLGAGAMFPPTSIYHVFQSRKDCVDPCGP                            448
hRFT1sv  167 --------------------------------                              167
rRFT1    416 .........V.......V.P..R.GE....Q...                          450
```

B

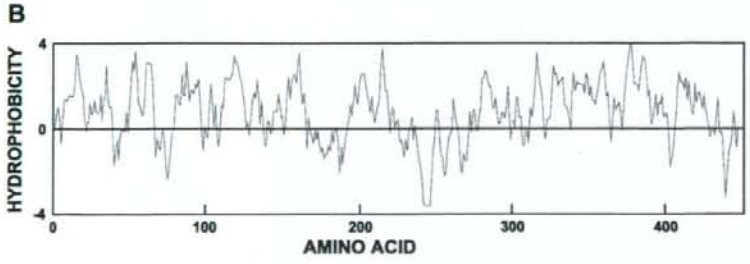

C

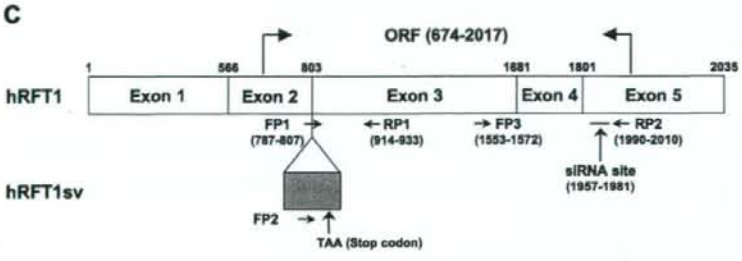

Fig. 1. *A*: comparison of the deduced amino acid sequences of human riboflavin transporter 1 (hRFT1), splice variant of hRFT1 (hRFT1sv), and rat RFT1 (rRFT1). The conserved residues in hRFT1 are indicated by dots. The GenBank accession numbers for hRFT1, hRFT1sv, and rRFT1 are AB362533, AB362534, and AB362535, respectively. *B*: hydropathy plot of hRFT1. *C*: cDNA sequences of hRFT1 and hRFT1sv. FP1, FP2, FP3, RP1, and RP2 are forward or reverse primers specific for hRFT1 or hRFT1sv, as shown in MATERIALS AND METHODS. ORF is open reading frame of hRFT1. siRNA, small interfering RNA.

These genes were subcloned into the plasmid vector pBK-CMV or pEGFP-C1.

Cell culture and transfection. HEK-293 cells (American Type Culture Collection CRL-1573) were cultured in complete medium consisting of Dulbecco's modified Eagle's medium (Sigma Chemical, St. Louis, MO) supplemented with 10% fetal bovine serum (Invitrogen, Carlsbad, CA) in an atmosphere of 5% CO_2-95% air at 37°C. The human colon carcinoma cell line Caco-2, obtained from the American Type Culture Collection (ATCC HTB37) was cultured in complete medium consisting of Dulbecco's modified Eagle's medium, supplemented with 10% fetal bovine serum and 1% nonessential amino acids (Invitrogen).

For a transient expression system, pBK-CMV and pEGFP-C1 containing hRFT1, hRFT1sv, and rRFT1 were purified using the Midi-V100TM Ultrapure Plasmid Extraction System (Viogene, Sunnyvale, CA). For the RNA interference system, the sequence of small interfering RNA (siRNA) targeting hRFT1 and hRFT1sv was as follows: 5′-UCCCACCAGCAUCUACCACGUGUUU-3′ (Fig. 1*C*). A nonspecific siRNA with the same guanine-cytosine content was used as a control: 5′-UCCGACCCUACCCAUUGCAGACUUU-3′. The siRNAs were synthesized by Invitrogen. On the day before the transfection, the cells were seeded onto poly-D-lysine-coated 24-well plates at a density of 5×10^4 cells per well. The cells were transfected with 200 ng per well of plasmid DNA or 20 pmol per well of siRNA using 1 μl of LipofectAMINE 2000 (Invitrogen) per well according to the manufacturer's instructions. Forty-eight hours after the transfection, the cells were used for the subsequent experiments.

Reverse transcription-PCR and real-time PCR. Total RNA (1 μg) from human tissues (fetal brain, fetal liver, adrenal gland, bone marrow, cerebellum, whole brain, heart, kidney, colon, lung, placenta, salivary gland, skeletal muscle, spleen, testis, uterus, thymus, small intestine, stomach, and liver) obtained from BioChain (Hayward, CA), rat tissues (brain, heart, lung, liver, small intestine, spleen, kidney cortex, and kidney medulla) from BioChain, and cells (HEK-293 cells and Caco-2 cells) were reverse transcribed with random hexamers, using Superscript II reverse transcriptase (Invitrogen), and were then digested with RNase H (Invitrogen). The resulting single-stranded DNA fragments were amplified with a forward primer 5′-TACCTCTCAGTGCTTGTGGCA-3′ and a reverse primer 5′-TGGCTCCTGCAATGGTGA-3′ specific for rRFT1, with a forward primer 5′-AAAAGACCTTCCAGAGGGTTG-3′ (FP1) and a reverse primer 5′-AGCACCTGTACCACCTGGAT-3′ (RP1) specific for hRFT1, and with a forward primer 5′-ACATGGCATCATTCCTTCCCT-3′ (FP2) and a reverse primer 5′-AGCACCTGTACCACCTGGAT-3′ (RP1) specific for hRFT1sv (Fig. 1*C*). To examine the effect of siRNA on the sum of the mRNA expression of hRFT1 and hRFT1sv, we used a forward primer 5′-AATGGCGTGCTGCCTTCTGT-3′ (FP3) and a reverse primer 5′-CAGGGGTCTACACAGTCCTTT-3′ (RP2) specific for hRFT1 and hRFT1sv (Fig. 1*C*). The PCR products were separated by 2% agarose gel electrophoresis and visualized by ethidium bromide staining. To determine the sum of the mRNA expression of hRFT1 and hRFT1sv, real-time PCR was carried out as described previously (28).

Western blot analysis. Cell lysate was directly prepared from the cells with 1% NP-40, and crude membrane fractions were prepared as described previously, with some modifications (42). Briefly, cells were homogenated by sonication in the buffer (250 mM sucrose and 5 mM HEPES, pH 7.4) and were then centrifuged (2,000 *g*, 10 min). The supernatant was recentrifuged (15,000 *g*, 30 min), and the pellet was used for the crude membrane samples. Cell lysate fractions (75 μg) and crude membrane fractions (25 μg) were separated by 10% sodium dodecyl sulfate-polyacrylamide gel electrophoresis and were transferred onto polyvinylidene difluoride membranes (Immobilon-P; Millipore, Bedford, MA) by semi-dry electroblotting. The blots were

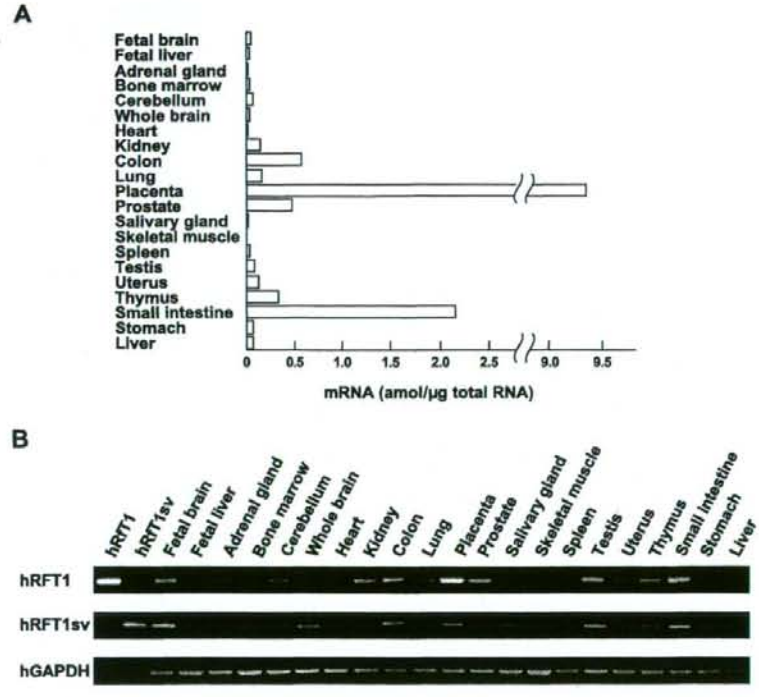

Fig. 2. Real-time PCR (*A*) and the splice variant-specific RT-PCR analysis (*B*) of hRFT1 and hRFT1sv are shown. *A*: mRNA level of hRFT1 and hRFT1sv determined by real-time PCR. The mRNA level of hRFT1 was calculated by the absolute standard method. The primer and probe set for hRFT1 cross-reacted with both hRFT1 and hRFT1sv. Therefore, the data represent the mRNA levels of both hRFT1 and hRFT1sv. *B*: RT-PCR amplification of hRFT1 and hRFT1sv mRNAs with specific primer sets. The PCR products of 126 bp and 154 bp correspond to hRFT1 and hRFT1sv, respectively. The quality of the RNA samples was also checked by RT-PCR for GAPDH as an internal control. Plasmid DNAs encoding hRFT1 and hRFT1sv were used as a positive control for hRFT1 and hRFT1sv.

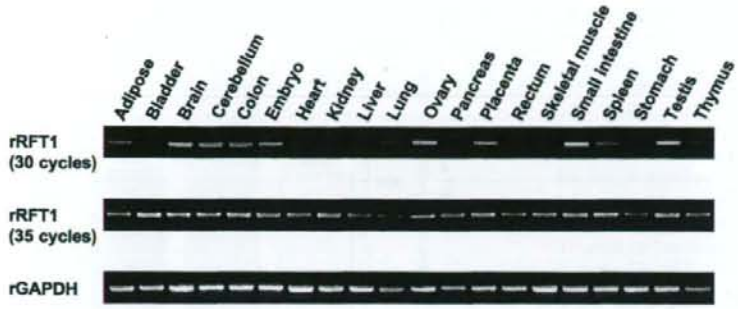

Fig. 3. RT-PCR analysis for the detection of rRFT1 mRNA. Total RNA isolated from various rat tissues was reverse transcribed and RT-PCR amplified for 30 or 35 cycles with the specific primer set for rRFT1. The PCR product of 626 bp corresponds to rRFT1. The quality of the RNA samples was also checked by RT-PCR of GAPDH as an internal control.

blocked and incubated overnight at 4°C with a primary antibody specific for green fluorescent protein (GFP; Roche Diagnostics, Indianapolis, IN). The bound antibody was detected on X-ray film using enhanced chemiluminescence with horseradish peroxidase-conjugated secondary antibodies and cyclic diacylhydrazides (GE Healthcare UK, Little Chalfont, United Kingdom).

Fluorescence cytochemistry. HEK-293 cells were transfected with the plasmid vector pEGFP-C1 containing rRFT1, hRFT1, or hRFT1sv as described above. The cells were fixed with 4% paraformaldehyde for 30 min at room temperature and observed using a BX-50-FLA fluorescence microscope (Olympus, Tokyo, Japan). Images were captured with a DP-50 CCD camera (Olympus) using Studio Lite software (Olympus).

Uptake experiment. Cellular uptake of [^{3}H]riboflavin (1.517 TBq/mmol; Moravek Biochemicals, Brea, CA), [*N*-methyl-^{3}H]cimetidine (451 GBq/mmol; GE Healthcare), [methyl-^{14}C]choline (2.035 GBq/mmol; American Radiolabeled Chemicals, St. Louis, MO), [6,7-^{3}H(*N*)]estrone-3-sulfate, ammonium salt ([^{3}H]ES; 2.1 TBq/mmol; PerkinElmer Life Analytical Sciences, Boston, MA), and [^{3}H (*G*)]thiamine (370 GBq/mmol; American Radiolabeled Chemicals) was measured with monolayer cultures grown on poly-D-lysine-coated 24-well plates. The composition of the incubation buffer was as follows: 145 mM NaCl, 3 mM KCl, 1 mM $CaCl_2$, 0.5 mM $MgCl_2$, 5 mM D-glucose, and 5 mM HEPES (pH was adjusted with NaOH). The Na^+-free incubation buffer was prepared by replacing Na^+ with *N*-methyl-D-glucamine or choline. The experimental procedures and the composition of other incubation buffers were described previously (43). Concentration dependence of riboflavin transport was fit by the combination of the Michaelis-Menten equation and a linear relationship: $V = V_{max}[S]/(K_m + [S]) + K_d[S]$, where V is transport rate, V_{max} is the maximal transport rate, $[S]$ is the concentration of riboflavin, K_m is Michaelis-Menten constant, and K_d is a diffusion constant.

The protein content of the cell monolayers solubilized in 0.5 N NaOH was determined by the method of Bradford with a Bio-Rad Protein Assay Kit (Bio-Rad Laboratories, Richmond, CA) with bovine γ-globulin as a standard.

Statistical analysis. Data are expressed as means ± SE. The data were analyzed statistically using an unpaired Student's *t*-test. Multiple comparisons were performed using Tukey's two-tailed test after a one-way analysis of variance. Probability values of less than 0.05 were considered statistically significant.

RESULTS

Isolation and structural analysis of hRFT1, hRFT1sv, and rRFT1. A single clone encoding rRFT1 was isolated and sequenced. The rRFT1 cDNA (GenBank accession no.

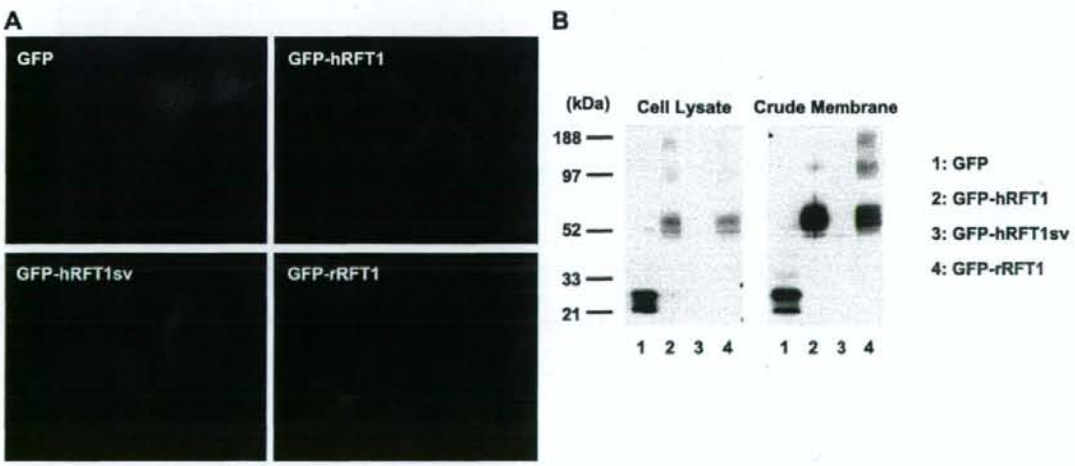

Fig. 4. Fluorescence cytochemistry and Western blot analysis of enhanced green fluorescent protein (EGFP)-tagged hRFT1, hRFT1sv, and rRFT1. *A*: human embryonic kidney (HEK)-293 cells transfected with EGFP-tagged hRFT1, hRFT1sv, and rRFT1. Cells were fixed with 4% paraformaldehyde and observed using a BX-50-FLA fluorescence microscope. *B*: Western blot analysis using the crude membrane of HEK-293 cells expressing EGFP-tagged hRFT1, hRFT1sv, and rRFT1.

AB362535) consists of 2,047 bp with an open reading frame encoding a 450-amino acid protein. It was predicted to have 10 putative membrane-spanning domains by the SOSUI program (10). There is a potential site for NH_2-linked glycosylation at position 178 and two consensus sequences for protein kinase COOH-dependent phosphorylation at positions 76 and 278 in rRFT1. Moreover, a human ortholog, hRFT1, and its splice variant, hRFT1sv, were isolated. The hRFT1 cDNA (GenBank accession no. AB362533) consists of 2,305 bp coding for a 448-amino acid protein with 81.1% amino acid identity and 96.4% similarity to rRFT1. It was also predicted to have 10 putative membrane-spanning domains (Fig. 1*B*). There is a potential site for NH_2-linked glycosylation at position 178 and a consensus sequence for protein kinase COOH-dependent phosphorylation at position 438 in hRFT1. The hRFT1sv cDNA (GenBank accession no. AB362534) consists of 2,402 bp coding for a 167-amino acid protein, possessing one putative membrane-spanning domain. The hRFT1 transcript consists of five exons (Fig. 1*C*). Unlike hRFT1, hRFT1sv was not spliced between exon 2 and exon 3 of hRFT1. Thus, an insertion of 118 bp between exon 2 and exon 3 of hRFT1 was found in hRFT1sv. The amino acid sequences of hRFT1, hRFT1sv, and rRFT1 are shown in Fig. 1*A*.

Tissue distribution, cellular localization, and functional characterization of hRFT1, hRFT1sv, and rRFT1. The mRNA levels of hRFT1 and hRFT1sv were examined at the mRNA level by real-time PCR as a sum of the expression of both mRNAs (Fig. 2*A*). The hRFT1 and hRFT1sv mRNAs were expressed strongly in the placenta and small intestine, moderately in the kidney, colon, lung, prostate, uterus, and thymus, and weakly in all other tissues. In addition, we separately detected hRFT1 and hRFT1sv in human tissues by RT-PCR using specific primer sets (Fig. 2*B*). PCR products of the size expected for hRFT1 and hRFT1sv (147 bp and 155 bp) were found in 21 human tissues; however, in some tissues (hRFT1: heart, skeletal muscle, stomach and liver; hRFT1sv: adrenal grand, prostate, spleen, and uterus), the signals were very weak. To rule out the contamination of genomic DNA, RT-PCR was carried out using the samples that were reverse transcribed with or without Superscript II reverse transcriptase (Supplemental Fig. 1; supplemental material for this article is available online at the *American Journal of Physiology-Cell Physiology* website). Moreover, the tissue distribution of rRFT1 was determined (Fig. 3). A PCR product of the size expected for rRFT1 was found in 20 rat tissues and especially highly in the adipose, brain, colon, ovary, placenta, small intestine, spleen, and testis.

To visualize the cellular localization of these proteins, HEK-293 cells were transfected with enhanced GFP (EGFP)-tagged hRFT1, hRFT1sv, and rRFT1 (Fig. 4*A*). Fluorescence was observed in the plasma membrane of the most cells transfected with EGFP-tagged hRFT1 and rRFT1. A weak signal from EGFP-tagged hRFT1sv was observed in the cytoplasm of only a few cells. In addition, Western blot analysis was performed using the cell lysate and crude membrane of HEK-293 cells transfected with these cDNAs (Fig. 4*B*). A signal for EGFP-tagged hRFT1 and rRFT1 was strongly detected in the crude membrane and weakly observed in the cell lysate. However, no signal for EGFP-tagged hRFT1sv was observed in the cell lysate and crude membrane.

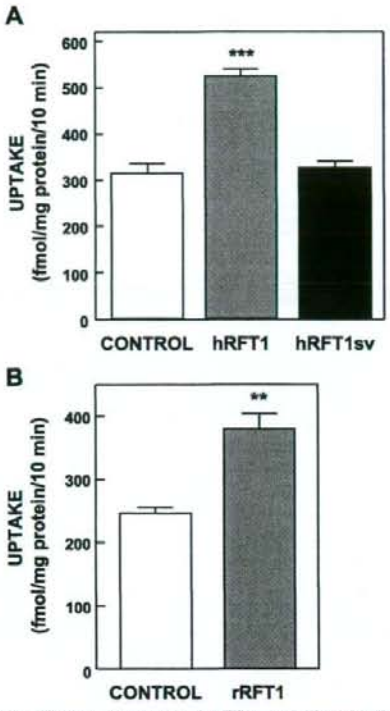

Fig. 5. Effect of hRFT1, hRFT1sv, and rRFT1 transfection on cellular uptake of [^{3}H]riboflavin. HEK-293 cells were transfected with empty vector (control), hRFT1, and hRFT1sv (*A*) and rRFT1 (*B*). The cells were incubated in incubation buffer containing 5 nM [^{3}H]riboflavin for 10 min at 37°C. Each bar represents the mean ± SE of three wells. $^{**}P = 0.006$, $^{***}P < 0.001$, significantly different from vector-transfected cells.

We screened more than 25 compounds and identified riboflavin as a substrate for RFT1 (Fig. 5 and Supplemental Table). The uptake of [^{3}H]riboflavin was significantly increased by the transfection with hRFT1 cDNA, but not with hRFT1sv cDNA (Fig. 5*A*). Moreover, uptake was also significantly increased in the rRFT1-transfected cells compared with control cells (Fig. 5*B*). In addition, uptake of [^{3}H]riboflavin by *Xenopus* oocytes expressing rRFT1 was also examined (Supplemental Fig. 2). Injection of rRFT1 cRNA into *Xenopus* oocytes tended to increase the uptake of [^{3}H]riboflavin compared with water-injected oocytes, but this increase was not significant. In the presence of 0.1 mM unlabeled riboflavin, uptake of [^{3}H]riboflavin by *Xenopus* oocytes was almost completely suppressed.

Uptake of [^{3}H]riboflavin by HEK-293 cells. Before the riboflavin transport activity of the native transporter was evaluated, the mRNA expression of hRFT1 and hRFT1sv was examined. RT-PCR products of a size expected for hRFT1 and hRFT1sv corresponding to the positive controls were found in HEK-293 cells corresponding to positive controls (Fig. 6). Therefore, it is suggested that the [^{3}H]riboflavin transport activity in HEK-293 cells is mediated, at least in part, by hRFT1. The functional characterization of riboflavin transport by HEK-293 cells was carried out. The uptake of [^{3}H]ribofla-

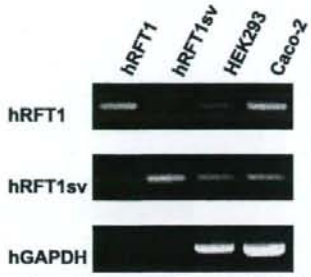

Fig. 6. RT-PCR analysis of hRFT1 and hRFT1sv. Total RNA isolated from HEK-293 cells and Caco-2 cells was reverse transcribed and RT-PCR amplified with specific primer sets for hRFT1 and hRFT1sv. The PCR products of 126 bp and 154 bp correspond to hRFT1 and hRFT1sv, respectively. The quality of the RNA samples was also checked by RT-PCR of GAPDH as an internal control. Plasmid DNAs encoding hRFT1 and hRFT1sv were used as a positive control for hRFT1 and hRFT1sv.

vin in HEK-293 cells increased in a time-dependent manner (Fig. 7*A*). The replacement of Na^+ with *N*-methyl-D-glucamine or choline did not affect the [^{3}H]riboflavin uptake by HEK-293 cells (Fig. 7*B*). The [^{3}H]riboflavin uptake was not changed in the presence of high K^+, Ba^{2+}, valinomycin, or high K^+ and valinomycin (Fig. 7*C*). Moreover, the pH dependence was not observed (Fig. 7*D*). In the presence of riboflavin analogues, FAD, FMN, and lumiflavin, uptake of [^{3}H]riboflavin by HEK-293 cells was decreased. On the other hand, probenecid or cimetidine did not influence the [^{3}H]riboflavin uptake (Fig. 7*E*). To clarify whether the native [^{3}H]riboflavin transport activity in HEK-293 cells corresponded to hRFT1, the influence of siRNA specific for hRFT1 and hRFT1sv (hRFT1/hRFT1sv siRNA) was examined. Transfection of control siRNA into HEK-293 cells did not affect the uptake of [^{3}H]riboflavin compared with nontransfected cells [261.1 ± 4.8 fmol·mg protein^{-1}·10 min^{-1} (nontransfected) vs. 256.7 ± 2.6 fmol·mg protein^{-1}·10 min^{-1} (control siRNA); $P = 0.12$]. The uptake of [^{3}H]riboflavin was significantly decreased after the transfection with hRFT1/hRFT1sv siRNA (Fig. 8*A*). RT-PCR analysis confirmed that hRFT1/hRFT1sv siRNA reduced the sum of hRFT1 and hRFT1sv mRNA expression (Fig. 8*B*). A saturable concentration-dependent uptake of [^{3}H]riboflavin by HEK-293 cells transfected with hRFT1/hRFT1sv siRNA or control siRNA was observed (Fig. 8*C*). In addition, the apparent Michaelis-Menten constant (K_m) and maximal uptake rate

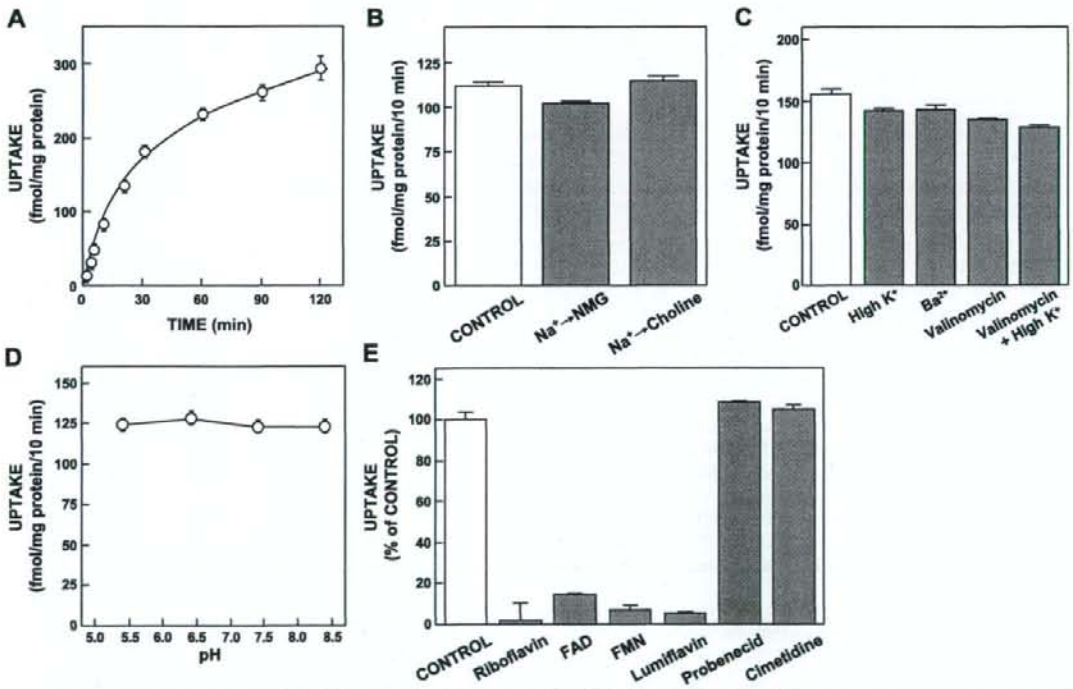

Fig. 7. Uptake of [^{3}H]riboflavin by HEK-293 cells. *A*: time-dependent uptake of [^{3}H]riboflavin by HEK-293 cells. Cells were incubated in incubation buffer (pH 7.4) containing 5 nM [^{3}H]riboflavin for various periods at 37°C. *B*: Na^+ dependence of uptake by HEK-293 cells. In the Na^+-free incubation medium, Na^+ was replaced with *N*-methyl-D-glucamine (NMG) or choline. *C*: membrane potential dependence of uptake by HEK-293 cells. The cells were incubated in the high K^+ (3 mM Na^+ and 145 mM K^+), Ba^{2+}, valinomycin (10 μM), or valinomycin and high K^+-present incubation buffer (pH 7.4) containing 5 nM [^{3}H]riboflavin for 10 min at 37°C. *D*: pH dependence of [^{3}H]riboflavin uptake by HEK-293 cells. The cells were incubated in incubation buffer (pH 5.4–8.4) containing 5 nM [^{3}H]riboflavin for 10 min at 37°C. *E*: the inhibitory effect of riboflavin analogues (0.1 mM), probenecid (1 mM), and cimetidine (1 mM) on the [^{3}H]riboflavin uptake by HEK-293 cells. The cells were incubated in incubation buffer (pH 7.4) containing 5 nM [^{3}H]riboflavin in the presence of inhibitors for 10 min at 37°C. Each point and bar represents the mean ± SE of three wells. FAD, flavin adenine dinucleotide; FMN, flavin mononucleotide.

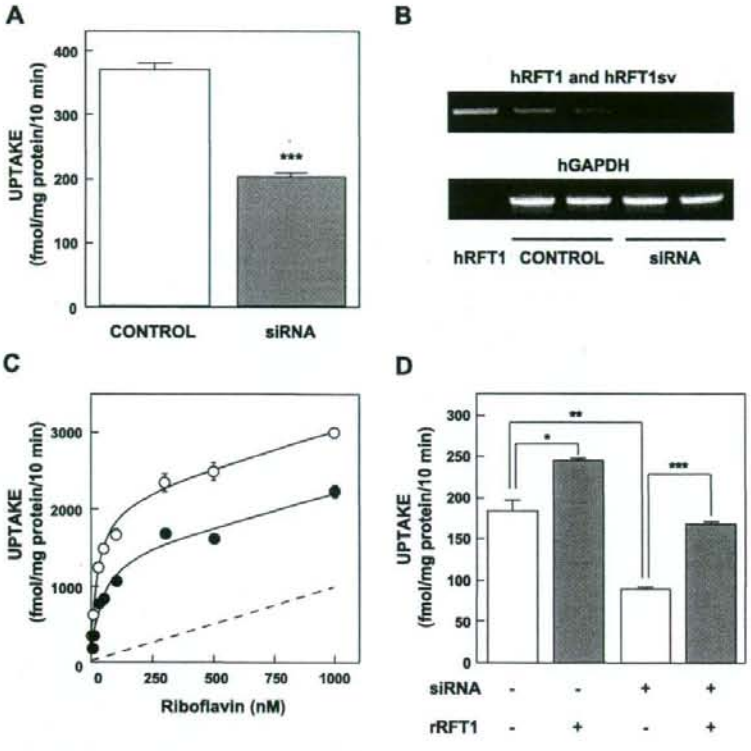

Fig. 8. Effect of siRNA for hRFT1 on the [^{3}H]riboflavin uptake by HEK-293 cells. *A*: uptake of [^{3}H]riboflavin by HEK-293 cells transfected with control siRNA (control) or siRNA for hRFT1 and hRFT1sv (siRNA). The cells were incubated in incubation buffer (pH 7.4) containing 5 nM [^{3}H]riboflavin for 10 min at 37°C. $***P < 0.001$, significantly different from control siRNA-transfected cells. *B*: RT-PCR amplification of hRFT1 and hRFT1sv mRNAs in HEK-293 cells transfected with hRFT1/hRFT1sv siRNA. The PCR product of 457 bp corresponds to hRFT1 and hRFT1sv. The quality of the RNA samples was also checked by RT-PCR of GAPDH as an internal control. Plasmid DNAs encoding hRFT1 and hRFT1sv were used as a positive control for hRFT1 and hRFT1sv. *C*: concentration-dependent uptake of [^{3}H]riboflavin by HEK-293 cells transfected with control siRNA (○) or hRFT1/hRFT1sv siRNA (●). Cells were incubated in incubation buffer (pH 7.4) containing [^{3}H]riboflavin at various concentrations for 10 min at 37°C. Data were analyzed by Michaelis-Menten equation ($r^2 = 1$, $P < 0.001$ and 0.98, $P < 0.001$ for control siRNA and hRFT1/hRFT1sv siRNA, respectively). The dashed line is $K_d[S]$. *D*: uptake of [^{3}H]riboflavin by HEK-293 cells transfected with control siRNA or hRFT1/hRFT1sv siRNA and empty vector or rRFT1. The cells were incubated in incubation buffer containing 5 nM [^{3}H]riboflavin for 10 min at 37°C. $*P = 0.0104$, $**P = 0.0021$, $***P < 0.001$, significantly different.

(V_{max}) were compared between the cells transfected with hRFT1/hRFT1sv siRNA and those transfected with the control siRNA. The calculated K_m values were 28.1 ± 2.8 nM and 35.0 ± 4.1 nM ($P = 0.214$), respectively. Transfection with hRFT1/hRFT1sv siRNA significantly decreased the calculated V_{max} value (2,368.3 ± 109.0 vs. vs. 1,662.3 ± 94.2 fmol·mg protein^{-1}·10 min^{-1}; $P = 0.003$). We examined the ability of rRFT1 to rescue the knockdown by hRFT1 siRNA (Fig. 8*D*). Transfection of rRFT1 caused a 1.3-fold and 1.9-fold increase in the riboflavin uptake by control siRNA and hRFT1/hRFT1sv siRNA transfected cells, respectively. Moreover, substrate specificity was examined. The uptake of [^{3}H]cimetidine, [^{3}H]estrone sulfate, [^{3}H]choline, and [^{3}H]thiamine was unchanged in HEK-293 cells transfected with hRFT1/hRFT1sv siRNA, although the uptake of [^{3}H]riboflavin was significantly decreased (Fig. 9).

Uptake of [^{3}H]riboflavin by Caco-2 cells. Before the activity of the native transporter was evaluated, the mRNA expression of hRFT1 and hRFT1sv in Caco-2 cells was determined (Fig. 6). As shown in Fig. 10*A*, the uptake of [^{3}H]riboflavin increased in a concentration-dependent manner. The apparent K_m and V_{max} values were 63.7 ± 6.9 nM and 853.4 ± 52.7 fmol·mg protein^{-1}·10 min^{-1}, respectively. To clarify whether the native [^{3}H]riboflavin transport activity in Caco-2 cells corresponds to hRFT1, the influence of hRFT1/hRFT1sv siRNA was examined. The uptake of [^{3}H]riboflavin was significantly decreased after the transfection with hRFT1/hRFT1sv siRNA (Fig. 10*B*).

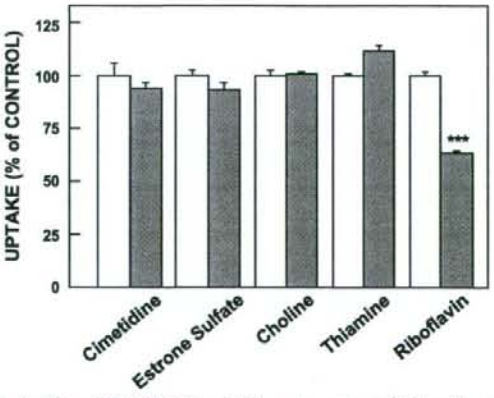

Fig. 9. Effect of hRFT1/hRFT1sv siRNA on the uptake of [^{3}H]cimetidine (23 nM), [^{3}H]estrone sulfate (19 nM), [^{14}C]choline (5 μM), [^{3}H]thiamine (14 μM), and [^{3}H]riboflavin (5 nM) by HEK-293 cells. HEK-293 cells were transfected with control siRNA (open bar) or hRFT1/hRFT1sv siRNA (shaded bar). The cells were incubated in incubation buffer (pH 7.4) containing radiolabeled compounds for 10 min at 37°C. Each bar represents the mean ± SE of three wells. $***P < 0.001$, significantly different from control siRNA-transfected cells.

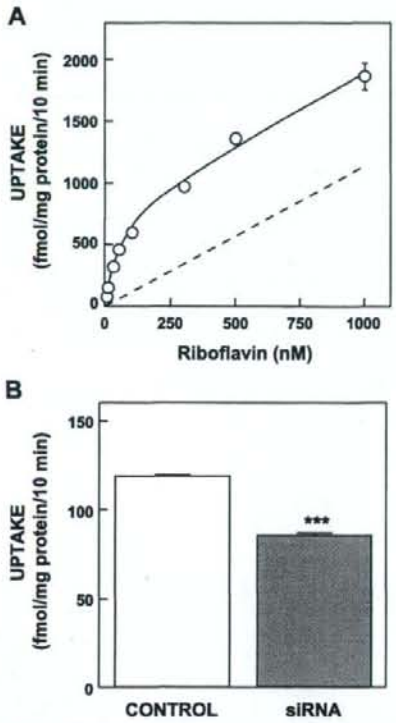

Fig. 10. Uptake of [^{3}H]riboflavin by Caco-2 cells. *A*: concentration-dependent uptake of [^{3}H]riboflavin by Caco-2 cells. Cells were incubated in incubation buffer (pH 7.4) containing [^{3}H]riboflavin at various concentrations for 10 min at 37°C. Data were analyzed by Michaelis-Menten equation ($r^2 = 1$, $P < 0.001$). The dashed line is $K_d[S]$. *B*: uptake of [^{3}H]riboflavin by Caco-2 cells transfected with control siRNA (control) or siRNA for hRFT1 and hRFT1sv (siRNA). The cells were incubated in incubation buffer (pH 7.4) containing 5 nM [^{3}H]riboflavin for 10 min at 37°C. Each point and bar represent the mean ± SE. of three wells. ***$P < 0.001$, significantly different from control siRNA-transfected cells.

DISCUSSION

In the present study, novel human and rat riboflavin transporters (hRFT1 and rRFT1) were successfully identified. The tissue distribution, cellular localization, and functional characterization of hRFT1 suggested that hRFT1 plays an important role in the cellular uptake of riboflavin. An inactive splice variant of hRFT1, hRFT1sv, was also cloned. The hRFT1sv cDNA contains a 118-bp insertion between exon 2 and exon 3 of hRFT1. Transfection of hRFT1sv in HEK-293 cells which natively express hRFT1 did not affect the riboflavin uptake (Fig. 5*A*). In addition, EGFP-tagged hRFT1sv was observed in the cytoplasm of only a few cells and was not detected by Western blot analysis (Fig. 4). These results suggested that hRFT1sv is not a membrane protein and that hRFT1sv is neither an active transporter nor a dominant negative. The physiological role of hRFT1sv remains unclear and should be examined in future studies.

Mammals are unable to synthesize riboflavin and thus must acquire it from exogenous sources. The absorption of riboflavin from foods takes place predominantly in the small intestine through an active carrier-mediated transport process (17, 24, 41). In addition, carrier-mediated absorption in the colon is thought to be important, because riboflavin is synthesized by bacterial metabolism in the colon (21, 44). The high levels of hRFT1 in the small intestine and colon suggest that hRFT1 mediates the absorption of riboflavin at these sites (Fig. 2). The apparent K_m value of riboflavin uptake by human intestinal brush-border membrane vesicles was 7.3 μM (34) and that by rat intestinal basolateral membrane vesicles was 5.0 μM (35). Previous studies have demonstrated apparent K_m values of 7.3 μM for riboflavin uptake by human intestinal brush border membrane vesicles (34), and 5.0 μM for uptake by rat intestinal basolateral membrane vesicles (35). Corresponding K_m values for uptake by intestinal cells are 63.7 nM in Caco-2 cells (the present study; Fig. 10*A*), 0.30 μM in Caco-2 cells (36), and 0.14 μM in NCM460 cells (37). The K_m values associated with intestinal membrane vesicles are higher than those of intestinal cell lines. In the present study, the uptake of riboflavin by Caco-2 cells was partially inhibited by hRFT1/hRFT1sv siRNA (Fig. 10*B*). The binding constant (K_d) for the rat intestinal brush-border membrane has been calculated to be 0.07 μM and 0.12 μM, suggesting that more than two binding sites exist in the brush-border membrane (2). In addition, the uptake of riboflavin by HEK-293 cells, whose riboflavin uptake was partially mediated by hRFT1 (Fig. 8*A*), was independent of Na^+, membrane potential, or pH (Fig. 7, *B–D*) and was completely inhibited by riboflavin analogues (Fig. 7*E*) as previously reported and discussed (36). These results and previous reports suggested that hRFT1 could play, at least in part, a role in the absorption of riboflavin in the intestine as a high affinity transporter.

We previously constructed a rat kidney mRNA expression database by sequencing cDNA clones randomly selected from a rat kidney cDNA library (12). This database included 2,048 genes, most of which are abundantly expressed and physiologically significant in the kidney. There are 61 transporters (3.7% of the 1,666 known-function genes) including organic ion transporters (OAT1, OAT3, and OCTN2), Na^+-coupled phosphate cotransporter II (NaPi-IIa and NaPi-IIc), and aquaporin 2 (AQP2). These transporters have important physiological roles

Table 1. *hRFT1 homologs registered in the GenBank database: identity and similarity to hRFT1*

Species	Accession No.	Identity, %	Similarity, %
Homo sapiens (human; hRFT1)	AB362533	100	100
Pan troglodytes (chimpanzee)	XP_523560	99	100
Papio hamadryas (hamadryas baboon)	AAL59884	96	100
Macaca mulatta (rhesus monkey)	XP_001099620	97	100
Equus caballus (horse)	XP_001505049	88	98
Sus scrofa (pig)	NP_001004033	85	97
Bos taurus (cattle)	NP_001069369	85	97
Rattus norvegicus (Norway rat; rRFT1)	AB362535	81	96
Canis lupus (dog)	XP_532355	86	96
Mus musculus (house mouse)	NP_083919	82	96
Monodelphis domestica (gray short-tailed opossum)	XP_001371785	69	91
Danio rerio (zebrafish)	NP_955950	51	86
Xenopus laevis (African clawed frog)	NP_001088340	53	84

hRFT1, human riboflavin transporter 1; rRFT1, rat riboflavin transporter 1.

in the kidney (8, 16, 29, 30). A recent update of this database revealed the characteristics of some unknown genes. We focused on transmembrane proteins and successfully identified NaGLT1, which mediates the tubular reabsorption of glucose and fructose (11, 13). In addition, this database includes a Slc5a8, which was characterized as a monocarboxylate transporter, and is thought to be a tumor suppressor (27, 31). Moreover, mouse Oatp5 was also identified (3). Therefore, this database represents a useful resource for identifying the physiologically important transporters in the kidney.

We have twice attempted to raise an antibody against hRFT1 but have not succeeded in obtaining a functional one. The same amino acid sequence of hRFT1 has already been registered as GPR172B (accession no. NP_001098047) in the GenBank database, although its substrates and physiological function have yet to be determined. In addition, this gene was previously reported to be the human ortholog of the porcine receptor for endogenous retrovirus A, which mediates the infection of the cells with porcine endogenous retrovirus (6). Because its amino acid sequence is similar to that of a G protein-coupled receptor family member and a multimembrane spanning protein, it is anticipated that it will be difficult to produce a functional antibody against hRFT1, as previously reported (9, 22, 39). In the present study, EGFP-tagged hRFT1 was expressed in the plasma membrane (Fig. 4), suggesting that hRFT1 mediates the transport of riboflavin across the plasma membrane. An antibody against hRFT1 will, however, reveal its detailed distribution in the tissues.

The RibU protein of *Lactobacillus lactis* was identified to be a bacterial riboflavin transporter containing five putative transmembrane domains (1, 5). Its homologues were identified among bacterial genes but not among mammalian genes (26). The Mch5p protein of *Saccharomyces cerevisiae* is an ortholog of the mammalian monocarboxylate transporter and has been reported to transport riboflavin; the transport of riboflavin by the mammalian monocarboxylate transporter has, however, not been assessed (33). hRFT1 and rRFT1 exhibit no significant similarity to RibU, Mch5p, or SLC families; therefore, mammalian riboflavin transporters (hRFT1 and rRFT1) appear to belong to a novel mammalian riboflavin transporter family and not to the bacterial riboflavin transporter family. A BLAST search of the GenBank database identified homologues of hRFT1 from the following mammalian, fish, and amphibian species: *Pan troglodytes*, *Macaca mulatta*, *Papio hamadryas*, *Canis lupus*, *Sus scrofa*, *Bos taurus*, *Equus caballus*, *Mus musculus*, *Monodelphis domestica*, *Xenopus laevis*, and *Danio rerio*. The mammalian genes exhibit high levels of identity (>69%) and similarity (>91%) to hRFT1 (Table 1). On the basis of these results, it is suggested that these genes should be classified into a novel mammalian riboflavin transporter family.

In conclusion, hRFT1 and rRFT1 were identified and characterized as novel mammalian riboflavin transporters using our rat kidney mRNA expression database (12). In addition, an inactive splice variant, hRFT1sv, was cloned. RFT1 could play an important role in the homeostasis of riboflavin.

GRANTS

This study was supported in part by a grant-in-aid for Research on Advanced Medical Technology from the Ministry of Health, Labour and Welfare of Japan; by the Japan Health Science Foundation "Research on Health Sciences Focusing on Drug Innovation"; by a grant-in-aid for Scientific Research from the Ministry of Education, Science, Culture and Sports of Japan; and by the 21st Century Center of Excellence program "Knowledge Information Infrastructure for Genome Science."

REFERENCES

1. **Burgess CM, Slotboom DJ, Geertsma ER, Duurkens RH, Poolman B, van Sinderen D.** The riboflavin transporter RibU in *Lactococcus lactis*: molecular characterization of gene expression and the transport mechanism. *J Bacteriol* 188: 2752–2760, 2006.
2. **Casirola D, Gastaldi G, Ferrari G, Kasai S, Rindi G.** Riboflavin uptake by rat small intestinal brush border membrane vesicles: a dual mechanism involving specific membrane binding. *J Membr Biol* 135: 217–223, 1993.
3. **Choudhuri S, Ogura K, Klaassen CD.** Cloning, expression, and ontogeny of mouse organic anion-transporting polypeptide-5, a kidney-specific organic anion transporter. *Biochem Biophys Res Commun* 280: 92–98, 2001.
4. **Daniel H, Wille U, Rehner G.** In vitro kinetics of the intestinal transport of riboflavin in rats. *J Nutr* 113: 636–643, 1983.
5. **Duurkens RH, Tol MB, Geertsma ER, Permentier HP, Slotboom DJ.** Flavin binding to the high affinity riboflavin transporter RibU. *J Biol Chem* 282: 10380–10386, 2007.
6. **Ericsson TA, Takeuchi Y, Templin C, Quinn G, Farhadian SF, Wood JC, Oldmixon BA, Suling KM, Ishii JK, Kitagawa Y, Miyazawa T, Salomon DR, Weiss RA, Patience C.** Identification of receptors for pig endogenous retrovirus. *Proc Natl Acad Sci USA* 100: 6759–6764, 2003.
7. **Foraker AB, Khantwal CM, Swaan PW.** Current perspectives on the cellular uptake and trafficking of riboflavin. *Adv Drug Deliv Rev* 55: 1467–1483, 2003.
8. **Forster IC, Hernando N, Biber J, Murer H.** Proximal tubular handling of phosphate: a molecular perspective. *Kidney Int* 70: 1548–1559, 2006.
9. **Grisshammer R, Tate CG.** Overexpression of integral membrane proteins for structural studies. *Q Rev Biophys* 28: 315–422, 1995.
10. **Hirokawa T, Boon-Chieng S, Mitaku S.** SOSUI: classification and secondary structure prediction system for membrane proteins. *Bioinformatics* 14: 378–379, 1998.
11. **Horiba N, Masuda S, Ohnishi C, Takeuchi D, Okuda M, Inui K.** Na^+-dependent fructose transport via rNaGLT1 in rat kidney. *FEBS Lett* 546: 276–280, 2003.
12. **Horiba N, Masuda S, Takeuchi A, Saito H, Okuda M, Inui K.** Gene expression variance based on random sequencing in rat remnant kidney. *Kidney Int* 66: 29–45, 2004.
13. **Horiba N, Masuda S, Takeuchi A, Takeuchi D, Okuda M, Inui K.** Cloning and characterization of a novel Na^+-dependent glucose transporter (NaGLT1) in rat kidney. *J Biol Chem* 278: 14669–14676, 2003.
14. **Huang SN, Swaan PW.** Involvement of a receptor-mediated component in cellular translocation of riboflavin. *J Pharmacol Exp Ther* 294: 117–125, 2000.
15. **Huang SN, Swaan PW.** Riboflavin uptake in human trophoblast-derived BeWo cell monolayers: cellular translocation and regulatory mechanisms. *J Pharmacol Exp Ther* 298: 264–271, 2001.
16. **Inui K, Masuda S, Saito H.** Cellular and molecular aspects of drug transport in the kidney. *Kidney Int* 58: 944–958, 2000.
17. **Jusko WJ, Levy G.** Absorption, metabolism, and excretion of riboflavin-5′-phosphate in man. *J Pharm Sci* 56: 58–62, 1967.
18. **Jusko WJ, Levy G.** Pharmacokinetic evidence for saturable renal tubular reabsorption of riboflavin. *J Pharm Sci* 59: 765–772, 1970.
19. **Jusko WJ, Levy G, Yaffe SJ, Gorodischer R.** Effect of probenecid on renal clearance of riboflavin in man. *J Pharm Sci* 59: 473–477, 1970.
20. **Kansara V, Pal D, Jain R, Mitra AK.** Identification and functional characterization of riboflavin transporter in human-derived retinoblastoma cell line (Y-79): mechanisms of cellular uptake and translocation. *J Ocul Pharmacol Ther* 21: 275–287, 2005.
21. **Kasper H.** Vitamin absorption in the colon. *Am J Proctol* 21: 341–345, 1970.
22. **Kremer L, Marquez G.** Generation of monoclonal antibodies against chemokine receptors. *Methods Mol Biol* 239: 243–260, 2004.
23. **Kumar CK, Yanagawa N, Ortiz A, Said HM.** Mechanism and regulation of riboflavin uptake by human renal proximal tubule epithelial cell line HK-2. *Am J Physiol Renal Physiol* 274: F104–F110, 1998.
24. **Levy G, Jusko WJ.** Factors affecting the absorption of riboflavin in man. *J Pharm Sci* 55: 285–289, 1966.
25. **Lowy RJ, Spring KR.** Identification of riboflavin transport by MDCK cells using quantitative fluorescence video microscopy. *J Membr Biol* 117: 91–99, 1990.

26. **Mansour NM, Sawhney M, Tamang DG, Vogl C, Saier MH Jr.** The bile/arsenite/riboflavin transporter (BART) superfamily. *FEBS J* 274: 612–629, 2007.
27. **Miyauchi S, Gopal E, Fei YJ, Ganapathy V.** Functional identification of SLC5A8, a tumor suppressor down-regulated in colon cancer, as a Na^+-coupled transporter for short-chain fatty acids. *J Biol Chem* 279: 13293–13296, 2004.
28. **Motohashi H, Sakurai Y, Saito H, Masuda S, Urakami Y, Goto M, Fukatsu A, Ogawa O, Inui K.** Gene expression levels and immunolocalization of organic ion transporters in the human kidney. *J Am Soc Nephrol* 13: 866–874, 2002.
29. **Nezu J, Tamai I, Oku A, Ohashi R, Yabuuchi H, Hashimoto N, Nikaido H, Sai Y, Koizumi A, Shoji Y, Takada G, Matsuishi T, Yoshino M, Kato H, Ohura T, Tsujimoto G, Hayakawa J, Shimane M, Tsuji A.** Primary systemic carnitine deficiency is caused by mutations in a gene encoding sodium ion-dependent carnitine transporter. *Nat Genet* 21: 91–94, 1999.
30. **Nielsen S, Agre P.** The aquaporin family of water channels in kidney. *Kidney Int* 48: 1057–1068, 1995.
31. **Paroder V, Spencer SR, Paroder M, Arango D, Schwartz S Jr, Mariadason JM, Augenlicht LH, Eskandari S, Carrasco N.** Na^+/monocarboxylate transport (SMCT) protein expression correlates with survival in colon cancer: molecular characterization of SMCT. *Proc Natl Acad Sci USA* 103: 7270–7275, 2006.
32. **Powers HJ.** Riboflavin (vitamin B2) health. *Am J Clin Nutr* 77: 1352–1360, 2003.
33. **Reihl P, Stolz J.** The monocarboxylate transporter homolog Mch5p catalyzes riboflavin (vitamin B2) uptake in *Saccharomyces cerevisiae*. *J Biol Chem* 280: 39809–39817, 2005.
34. **Said HM, Arianas P.** Transport of riboflavin in human intestinal brush border membrane vesicles. *Gastroenterology* 100: 82–88, 1991.
35. **Said HM, Hollander D, Mohammadkhani R.** Uptake of riboflavin by intestinal basolateral membrane vesicles: a specialized carrier-mediated process. *Biochim Biophys Acta* 1148: 263–268, 1993.
36. **Said HM, Ma TY.** Mechanism of riboflavine uptake by Caco-2 human intestinal epithelial cells. *Am J Physiol Gastrointest Liver Physiol* 266: G15–G21, 1994.
37. **Said HM, Ortiz A, Moyer MP, Yanagawa N.** Riboflavin uptake by human-derived colonic epithelial NCM460 cells. *Am J Physiol Cell Physiol* 278: C270–C276, 2000.
38. **Said HM, Wang S, Ma TY.** Mechanism of riboflavin uptake by cultured human retinal pigment epithelial ARPE-19 cells: possible regulation by an intracellular Ca^{2+}-calmodulin-mediated pathway. *J Physiol* 566: 369–377, 2005.
39. **Saitoh R, Ohtomo T, Yamada Y, Kamada N, Nezu J, Kimura N, Funahashi S, Furugaki K, Yoshino T, Kawase Y, Kato A, Ueda O, Jishage K, Suzuki M, Fukuda R, Arai M, Iwanari H, Takahashi K, Sakihama T, Ohizumi I, Kodama T, Tsuchiya M, Hamakubo T.** Viral envelope protein gp64 transgenic mouse facilitates the generation of monoclonal antibodies against exogenous membrane proteins displayed on baculovirus. *J Immunol Methods* 322: 104–117, 2007.
40. **Spector R.** Riboflavin transport by rabbit kidney slices: characterization and relation to cyclic organic acid transport. *J Pharmacol Exp Ther* 221: 394–398, 1982.
41. **Stripp B.** Intestinal absorption of riboflavin by man. *Acta Pharmacol Toxicol (Copenh)* 22: 353–362, 1965.
42. **Terada T, Saito H, Mukai M, Inui K.** Identification of the histidine residues involved in substrate recognition by a rat H^+/peptide cotransporter, PEPT1. *FEBS Lett* 394: 196–200, 1996.
43. **Urakami Y, Kimura N, Okuda M, Inui K.** Creatinine transport by basolateral organic cation transporter hOCT2 in the human kidney. *Pharm Res* 21: 976–981, 2004.
44. **Yuasa H, Hirobe M, Tomei S, Watanabe J.** Carrier-mediated transport of riboflavin in the rat colon. *Biopharm Drug Dispos* 21: 77–82, 2000.
45. **Zempleni J, Galloway JR, McCormick DB.** Pharmacokinetics of orally and intravenously administered riboflavin in healthy humans. *Am J Clin Nutr* 63: 54–66, 1996.

0090-9556/08/3611-2299–2306$20.00
DRUG METABOLISM AND DISPOSITION
Vol. 36, No. 11
23168/3398205
Printed in U.S.A.

DMD 36:2299–2306, 2008

DMD
DRUG METABOLISM AND DISPOSITION

Significance of Organic Cation Transporter 3 (*SLC22A3*) Expression for the Cytotoxic Effect of Oxaliplatin in Colorectal Cancer[S]

Sachiko Yokoo, Satohiro Masuda, Atsushi Yonezawa, Tomohiro Terada, Toshiya Katsura, and Ken-ichi Inui

Department of Pharmacy, Kyoto University Hospital, Faculty of Medicine, Sakyo-ku, Kyoto, Japan

Received June 28, 2008; accepted August 14, 2008

ABSTRACT:

The effect of oxaliplatin against colorectal cancer is superior to that of cisplatin, but the molecular mechanism(s) involved is not clear. We found previously that oxaliplatin, but not cisplatin, was transported by human (h) and rat organic cation transporter 3 (OCT3)/*SLC22A3*. In the present study, we examined whether hOCT3 was significantly involved in the oxaliplatin-induced cytotoxicity and accumulation of platinum in colorectal cancer. The level of hOCT3 mRNA in the colon was 9.7-fold higher in cancerous than in normal tissues in six Japanese patients ($P = 0.0247$). In human colorectal cancer-derived cell lines, the mRNA of hOCT3 was highly expressed compared with that of other organic cation transporters. The release of lactate dehydrogenase (LDH) and accumulation of platinum with oxaliplatin treatment were increased in SW480 cells transfected with hOCT3 cDNA compared with empty vector-transfected cells. T84 and SW837 cells, with high levels of hOCT3, released more LDH and accumulated more platinum after oxaliplatin treatment than low hOCT3-expressing cells such as SW480, HCT116, HT29, and Lovo. However, the amount of platinum accumulated after cisplatin treatment did not differ among these six cell lines. The levels of hOCT3 expression in colon and rectum were also higher in cancerous than in normal tissues in Caucasian patients as determined by dot blotting. In conclusion, the hOCT3-mediated uptake of oxaliplatin into the cancers was suggested to be important for its cytotoxicity, and hOCT3 expression may be a marker for cancer chemotherapy including oxaliplatin.

Platinum agents are widely used in the treatment of cancers. *Cis*-diamminedichloroplatinum II (cisplatin) was the first platinum agent to be synthesized and has played an essential role in cancer chemotherapy for 30 years. However, severe nephrotoxicity and an increase in resistance to cisplatin therapy limit continuous clinical use. *Trans*-L-1,2-diaminocyclohexaneoxalatoplatinum II (oxaliplatin) is a third-generation platinum agent, which is less nephrotoxic than cisplatin. Moreover, its spectrum of activity and mechanisms of action or resistance differ from those of cisplatin (Raymond et al., 2002; Fuertes et al., 2003; Wang and Lippard, 2005). Oxaliplatin is used against colorectal cancers as a key drug in FOLFOX regimens, and its objective response rate for colorectal cancer is superior to that of cisplatin (Loehrer et al., 1988; Grem et al., 1993; de Gramont et al., 2000; Andre et al., 2004). However, the molecular mechanism(s) underlying the clinical results and that reason that oxaliplatin has such a potent anticolorectal cancer effect compared with cisplatin are unclear.

The organic cation transporters (OCT/*SLC22A*) and multidrug and toxin extrusion (MATE/*SLC47A*) family transport cationic drugs, toxins, and endogenous metabolites (Inui et al., 2000; Terada and Inui, 2008). Previously, we determined that the severity of the nephrotoxicity of platinum agents depends on the amount of platinum accumulated in the kidney, and OCT and MATE could play predominant roles in the renal handling of these agents (Yonezawa et al., 2005, 2006; Yokoo et al., 2007). We also reported that oxaliplatin, but not cisplatin, was selectively transported by rat (r) or human (h) organic cation transporter 3 (OCT3/*SLC22A3*) (Yonezawa et al., 2006; Yokoo et al., 2007). OCT3 mRNA was found in placenta, intestine, heart, brain, and kidney, but the distribution in the membrane and physiological role of OCT3 are not yet clearly understood (Kekuda et al., 1998).

We hypothesized that the substrate specificity and expression level of OCT3 affect the difference in the anticancer effect of platinum agents against colorectal cancer. In the present study, we examined

This work was supported in part by a grant-in-aid for Research on Biological Markers for New Drug Development, Health and Labour Sciences Research Grants from the Ministry of Health, Labour and Welfare of Japan, by the Mochida Memorial Foundation for Medical and Pharmaceutical Research, and by a grant-in-aid for Scientific Research from the Ministry of Education, Science, Culture and Sports of Japan.

Article, publication date, and citation information can be found at http://dmd.aspetjournals.org.

doi:10.1124/dmd.108.023168.

[S] The online version of this article (available at http://dmd.aspetjournals.org) contains supplemental material.

ABBREVIATIONS: cisplatin, *cis*-diamminedichloroplatinum II; oxaliplatin, *trans*-L-1,2-diaminocyclohexaneoxalatoplatinum II; FOLFOX, folinic acid (leucovorin), 5-fluorouracil, and oxaliplatin; OCT, organic cation transporter; MATE, multidrug and toxin extrusion; r, rat; h, human; DMEM, Dulbecco's modified Eagle's medium; FBS, fetal bovine serum; MPP, 1-methyl-4-phenylpyridium acetate; ICP-MS, inductively coupled plasma-mass spectrometry; LDH, lactate dehydrogenase; PCR, polymerase chain reaction; HEK, human embryonic kidney.

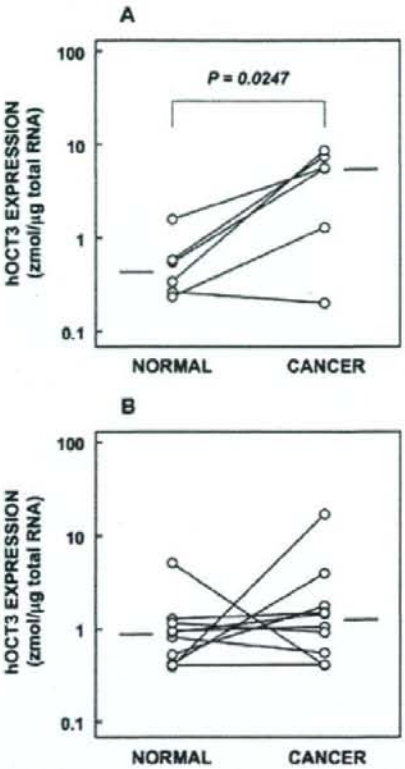

FIG. 1. hOCT3 mRNA expression in normal or cancerous tissues derived from Japanese patients. The expression of hOCT3 mRNA in colon (A) or rectum (B) was detected by real-time PCR. The numbers of patients with colon and rectum cancer were 6 and 10, respectively. The horizontal bars represent the median of hOCT3 mRNA expression.

and compared the levels of OCT3 mRNA in colorectal cancer and normal colorectum and among colorectal cancer-derived cell lines. In addition, the cytotoxicity and platinum accumulation in cultured cells caused by the treatment with oxaliplatin or cisplatin were examined.

Materials and Methods

Cell Culture. Human colorectal cancer-derived cell lines, T84 (CCL-248; American Type Culture Collection, Manassas, VA), SW480 (CCL-228; American Type Culture Collection), HCT116 (91091005; European Collection of Cell Cultures, Wiltshire, UK), HT29 (HTB-38; American Type Culture Collection), SW837 (JCRB9115; Health Science Research Resources Bank, Osaka, Japan), and Lovo (JCRB9083; Health Science Research Resources Bank) were used. Human embryonic kidney (HEK)293 cells (CRL-1573; American Type Culture Collection) were used as a host for gene transfection (Yonezawa et al., 2006). Cell lines were cultured in an atmosphere of 5% CO_2-95% air at 37°C. Dulbecco's modified Eagle's medium (DMEM) (Sigma-Aldrich, St. Louis, MO) with 10% fetal bovine serum (FBS) (Invitrogen, Carlsbad, CA) was used for SW480, HT29, HCT116, Lovo, and HEK293. DMEM containing 10% FBS and 1% nonessential amino acid (Invitrogen) was used for SW837, and a 1:1 mixture of DMEM and nutrient mixture Ham's F12 medium (Sigma-Aldrich) with 10% FBS was used for T84. T84, HT29, and Lovo cells were seeded onto 24-well plates or 96-well plates at a density of 4.0×10^5 cells/ml. SW480 and HCT116 cells were seeded at 2.0×10^5 cells/ml, and SW837 cells were seeded at 5.0×10^5 cells/ml. Seventy-two hours after the seeding, the cells were used for the experiments.

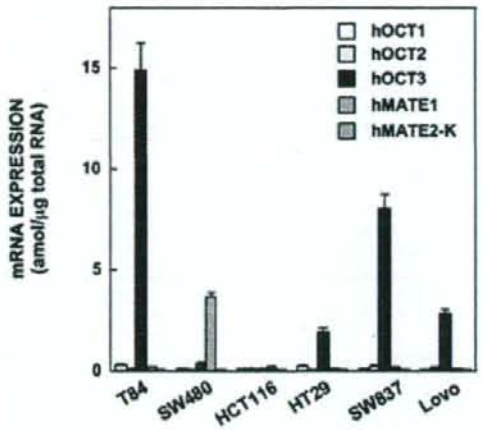

FIG. 2. mRNA levels of organic cation transporters in colorectal cancer-derived cell lines. Total RNA from the cell lines was reverse-transcribed, and the OCT1, hOCT2, hOCT3, hMATE1, or hMATE2-K expression levels were measured by using real-time PCR. Each column represents the mean ± S.E. for three wells. The plot of real-time PCR results for hOCT3 and glyceraldehyde-3-phosphate dehydrogenase is found in the supplemental data.

Transfection. For a transient expression system, pCMV6-XL4 plasmid vector DNA (OriGene Technologies, Rockville, MD) containing hOCT3 cDNA was purified using an EndoFree Plasmid Mega Kit (QIAGEN GmbH, Hilden, Germany) according to the manufacturer's instructions (Yonezawa et al., 2006). The day before transfection, HEK293 or SW480 cells were seeded onto poly-D-lysine-coated and noncoated 24-well plates, respectively. The cells were transfected with 800 ng of plasmid DNA per well in a combination of empty vector and hOCT3 cDNA using 2 μl of Lipofectamine 2000 (Invitrogen) per well according to the manufacturer's instructions. The amount of hOCT3 cDNA was 800 ng except in the experiment examining the transporter cDNA dependence. Forty-eight hours after the transfection, the cells were used for the experiments.

Uptake Experiment. Cellular uptake of [^{3}H]1-methyl-4-phenylpyridium acetate (MPP) (2.7 TBq/mmol; PerkinElmer Life and Analytical Sciences, Waltham, MA) was measured with monolayer cultures grown on 24-well plates. The composition of the incubation buffer was as follows: 145 mM NaCl, 3 mM KCl, 1 mM $CaCl_2$, 0.5 mM $MgCl_2$, 5 mM D-glucose, and 5 mM HEPES (pH 7.4 adjusted with NaOH). As previously reported, experiments on the uptake were performed (Urakami et al., 2004).

For measurement of the cellular accumulation of oxaliplatin or cisplatin, cells seeded on 24-well plates were incubated with DMEM containing 10% FBS and oxaliplatin (Wako Pure Chemical Industries, Osaka, Japan) or cisplatin (Sigma-Aldrich) for 2 min or 1 h. After this incubation, the monolayers were rapidly washed twice with ice-cold incubation buffer containing 3% bovine serum albumin (Nacalai Tesque, Kyoto, Japan) and then washed three times with ice-cold incubation buffer. The cells were solubilized in 0.5 N NaOH, and the amount of platinum was determined using inductively coupled plasma-mass spectrometry (ICP-MS) by the Pharmacokinetics and Bioanalysis Center, Shin Nippon Biomedical Laboratories, Ltd. (Wakayama, Japan). The protein content of the cell monolayers solubilized in 0.5 N NaOH was determined with a Bio-Rad Protein Assay Kit (Bio-Rad, Richmond, CA).

Cytotoxicity Assay. The cytotoxicity of oxaliplatin was measured with cells seeded on 24-well plates for the lactate dehydrogenase (LDH) assay and on 96-well plates for the caspase 3/7 assay. Cells were incubated with medium containing oxaliplatin for 6 h for the LDH assay. After removal of the medium, a drug-free medium was added to the wells. After incubation for 24 h, the medium was collected, and the LDH activity in it was measured using a LDH Cytotoxicity Detection Kit (Takara Bio Inc., Shiga, Japan), according to the manufacturer's instructions. LDH release (percent) was calculated as described previously (Yonezawa et al., 2006). For the caspase assay, cells were incubated

DMD DRUG METABOLISM AND DISPOSITION aspet

with medium containing oxaliplatin for 8 h. After the incubation, caspase 3/7 activity was determined by using a Caspase-Glo 3/7 Assay (Promega, Madison, WI), according to the manufacturer's instructions. Caspase activity (fold increase) represents (caspase 3/7 activity in oxaliplatin-treated cells)/(caspase 3/7 activity in cells without oxaliplatin).

Isolation of Total RNA and Real-Time PCR. Total RNA was isolated from each cell line on 24-well plates using an RNeasy Mini Kit (QIAGEN) according to the manufacturer's instructions, and the concentrations of total RNA were measured by spectrophotometry. Total RNA was reverse-transcribed with random hexamers using Superscript II reverse transcriptase (Invitrogen), followed by digestion with RNase H (Invitrogen). For the detection of the expression of hOCT3 mRNA in cancerous or normal colon and rectum, the same batch of cDNA samples as used by Terada et al. (2005) was subjected to real-time PCR. Detailed information about the patients was given in the report of Terada et al. (2005). The conditions and primer-probe sets for real-time PCR were described previously (Motohashi et al., 2002; Masuda et al., 2006). The glyceraldehyde-3-phosphate dehydrogenase mRNA level was used as an internal control. This study was conducted in accordance with the Declaration of Helsinki and its amendments and was approved by the Kyoto University Graduate School and Faculty of Medicine Ethics Committee.

Cancer Profiling Array. The cDNA cancer profiling array, Cancer Profiling Array I (Clontech, Mountain View, CA) was used. It includes normalized cDNAs from cancer and corresponding normal tissues from individual patients, amplified using SMART technology. Preparation of the cDNA probe for hOCT3, hybridization to the array, and signal detection on X-ray film were performed using the DIG High Prime DNA Labeling and Detection Starter Kit II (Roche Ltd., Basel, Switzerland) according to the manufacturer's instructions. The relative intensity of each dot was determined densitometrically using ImageJ 1.38x (National Institutes of Health, Bethesda, MD).

Statistical Analysis. Data are expressed as means ± S.E. Data were analyzed statistically using the paired Student's *t* test. Probability values of less than 0.05 were considered statistically significant.

Results

Expression of hOCT3 mRNA in Normal and Cancerous Colorectal Tissues. The expression of hOCT3 mRNA in colon ($n = 6$) or rectal ($n = 10$) tissue derived from Japanese patients was measured by real-time PCR. Figure 1 shows the difference in the expression between normal and cancerous colorectum. In cancerous colon tissue, the level of hOCT3 mRNA was significantly higher than that in normal tissue, and the mean increase in individuals was 9.7-fold (Fig. 1A). The median values of hOCT3 in normal and cancerous colon tissue were 0.44 (range 0.24–1.59) and 5.59 (range 0.20–8.62) zmol/μg of total RNA, respectively ($P = 0.0247$, by the paired Student's *t* test). hOCT3 mRNA expression in rectum tended to increase in cancerous tissue, but the difference was not significant (Fig. 1B). The median values of hOCT3 in normal and cancerous rectal tissue were 0.87 (range 0.39–5.17) and 1.26 (range 0.41–17.1) zmol/μg of total RNA, respectively ($P = 0.363$, by the paired Student's *t* test).

mRNA Expression of Organic Cation Transporters in Colorectal Cancer-Derived Cell Lines. We examined the expression of hOCT1, hOCT2, hOCT3, hMATE1, and hMATE2-K mRNA in colorectal cancer-derived cell lines, T84, SW480, HCT116, HT29, SW837, and Lovo, by real-time PCR. The hOCT3 transcript was found in all of these cells except HCT116 and was strongly detected in T84 and SW837 (Fig. 2). hMATE1 mRNA was only expressed in SW480. However, the mRNA expression of hOCT1, hOCT2, hMATE1, and hMATE2-K in these cells was almost negligible.

[^{3}H]MPP Uptake by Colorectal Cancer-Derived Cell Lines. To check the functional activity of hOCT3 in cultured cells, we measured the cellular uptake of its typical substrate, [^{3}H]MPP. The accumulation of [^{3}H]MPP was greater in T84 cells, SW480 cells expressing hOCT3, and HEK293 cells expressing hOCT3 than in SW480 cells, SW480 cells transfected with vector cDNA, and HEK293 cells transfected with vector cDNA (Fig. 3A). In addition, we examined [^{3}H]MPP uptake in other colorectal cancer-derived cell lines, HCT116, HT29, SW837, and Lovo. SW837 showed the highest level of activity to transport [^{3}H]MPP among these six cell lines (Fig. 3B). The transport activity of the cells was confirmed, and then these cells and expression systems were used in subsequent experiments on the cytotoxicity and the cellular transport of platinum agents.

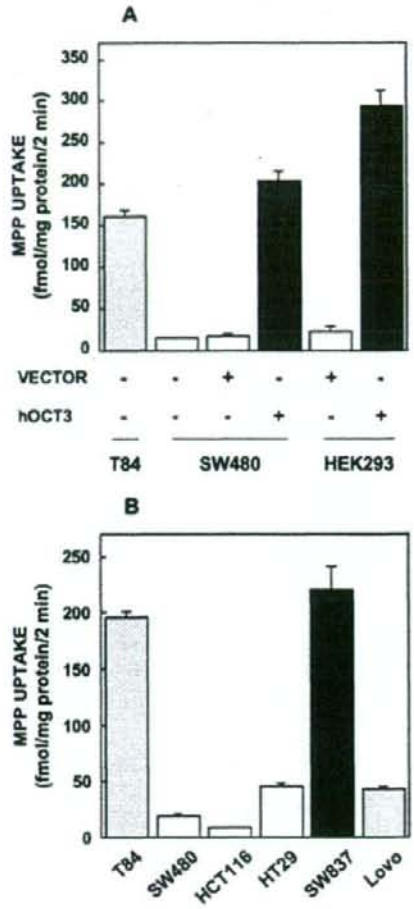

FIG. 3. Uptake of [^{3}H]MPP by colorectal cancer-derived cell lines or HEK293. After preincubation, native T84 or SW480 and SW480 cells or HEK293 cells transiently transfected with empty vector (vector) or hOCT3 cDNA (A), or T84, SW480, HCT116, HT29, SW837, or Lovo cells (B) were incubated with 13.7 nM [^{3}H]MPP for 2 min at 37°C. Each column represents the mean ± S.E. for three wells.

hOCT3 Expression and Oxaliplatin-Induced Cytotoxicity. We examined the effect of hOCT3 expression in a colon cancer-derived cell line, SW480. When SW480 cells transfected with 800 ng of empty vector or hOCT3 were treated with 500 μM oxaliplatin for 6 h and subsequently cultured in normal medium for 24 h, the release of LDH into the culture medium was increased by the expression of hOCT3 (Fig. 4A). In addition, we measured the amount of LDH released by treatment with 500 μM oxaliplatin in other colorectal cancer-derived cell lines. The amount of LDH released was greatest in

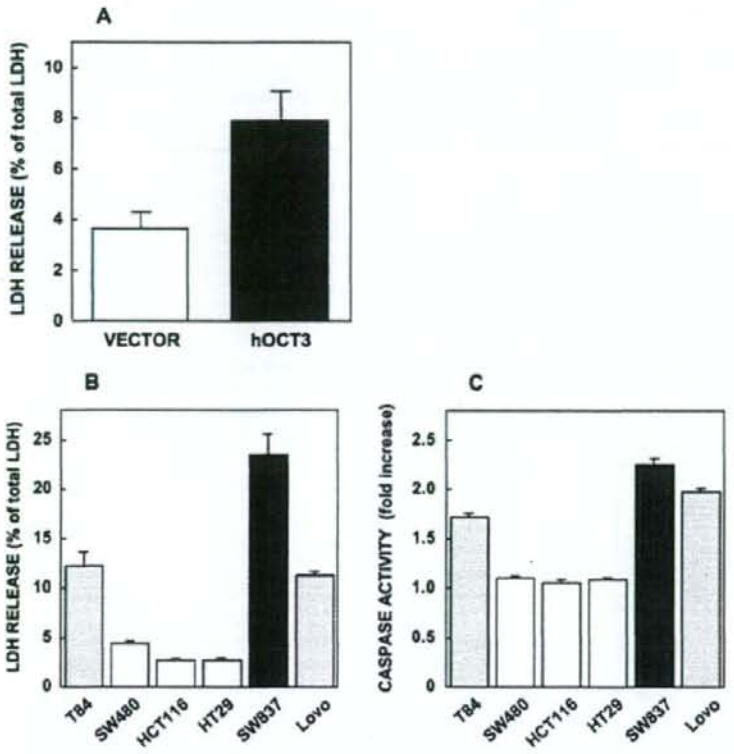

FIG. 4. Role of hOCT3 expression in oxaliplatin-induced cytotoxicity. SW480 cells transiently expressing hOCT3 or empty vector (A) or T84, SW480, HCT116, HT29, SW837, or Lovo cells (B) were treated with 500 μM oxaliplatin in the culture medium for 6 h. Then the cells were incubated in the normal culture medium for 24 h. The amount of LDH released into the medium was measured. C, T84, SW480, HCT116, HT29, SW837, or Lovo cells were treated with 50 μM oxaliplatin in the culture medium for 8 h, and then caspase 3/7 activity was measured. Each column represents the mean ± S.E. for three wells.

SW837 and was also large in T84 and Lovo cells (Fig. 4B). SW480, HCT116, and HT29 cells showed little release of LDH with oxaliplatin treatment.

In addition, caspase 3/7 activity induced by treatment with 50 μM oxaliplatin was examined in these cell lines. The most potent activation of caspase 3/7 was in SW837 but T84 and Lovo cells also showed strong caspase 3/7 activity (Fig. 4C). The results of caspase activity were consistent with those of LDH release.

Transport of Oxaliplatin. We examined the accumulation of oxaliplatin with the increase of hOCT3 cDNA on transfection of SW480 cells (Fig. 5A), because almost no hOCT3 mRNA was found in SW480 cells (Fig. 2). When SW480 cells transfected with 50 to 800 ng of hOCT3 cDNA per well were treated with 1000 μM oxaliplatin for 1 h, the level of platinum accumulated in the cells was increased, depending on the amount of hOCT3 cDNA transfected (Fig. 5A). Based on these results, we determined the platinum accumulation in T84 cells, SW480 cells, and SW480 cells transfected with 800 ng of hOCT3 cDNA. When treated with 100, 500, or 1000 μM oxaliplatin for 1 h, T84 cells and SW480 cells expressing hOCT3 transported oxaliplatin extensively in a concentration-dependent manner compared with SW480 cells or SW480 cells transfected with empty vector (Fig. 5B). Moreover, we examined the amount of platinum accumulated after the treatment with oxaliplatin in other colorectal cancer-derived cell lines, HCT116, HT29, SW837, and Lovo. Platinum was most abundant in SW837 cells at all three concentrations when the cells were incubated with the culture medium containing oxaliplatin for 2 min (Table 1). The same tendency was observed when they were treated for 1 h (Table 2). In HT29 and Lovo cells, the amount of platinum accumulated was approximately half of that in SW837 cells, and the levels in SW480 and HCT116 cells were low compared with those in other cultured cells.

Relation among hOCT3 mRNA Expression, LDH Release, and Platinum Accumulation. When cultured cells were treated with 500 μM oxaliplatin, the release of LDH was increased by the hOCT3 mRNA expression (Fig. 6A). The accumulation of platinum in the cells after the incubation with 500 μM oxaliplatin was also dependent on hOCT3 mRNA expression (Fig. 6B). By combining the data from Fig. 6, A and B, the release of LDH was also comparable with the accumulation of platinum (Fig. 6C). On the other hand, when cells were treated with 500 μM cisplatin, the accumulation of platinum was independent of hOCT3 mRNA expression (Fig. 6D).

Cancer Profiling Array. We examined the differences in hOCT3 expression between normal and cancerous tissues derived from Caucasians using dot blotting, and the density of each dot was quantified using ImageJ 1.38x (Fig. 7). In the colon, the level of hOCT3 was significantly higher in cancerous tissues (Fig. 7A). This result was consistent with that in Fig. 1A. A significant increase of hOCT3 expression was also observed in the rectum and stomach (Fig. 7, B and C). Inversely, a significant decrease of hOCT3 expression in cancerous tissue was detected in the uterus, breast, ovary, and lung (Fig. 7, D–G). In the kidney, there was no significant difference in hOCT3 mRNA expression between normal and cancerous tissue (Fig. 7H).

DRUG METABOLISM AND DISPOSITION DMD aspet

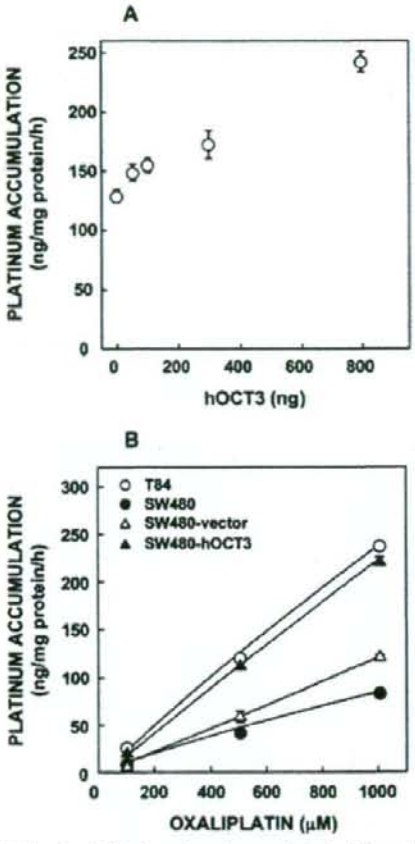

FIG. 5. Uptake of oxaliplatin by colorectal cancer-derived cell lines. A, SW480 cells were transfected with an amount of hOCT3 cDNA and vector plasmid added to 800 ng using 2 μl of Lipofectamine 2000. The cells were exposed to 1000 μM oxaliplatin in the culture medium for 1 h. B, T84 cells, SW480 cells, or SW480 cells transiently expressing empty vector or hOCT3 were treated with culture medium containing 100, 500, or 1000 μM oxaliplatin for 1 h. After being washed, these cells were solubilized in 0.5 N NaOH, and the amount of platinum was determined by ICP-MS. Each point represents the mean ± S.E. of four wells.

Discussion

Oxaliplatin has a much more potent anticolorectal cancer effect than cisplatin (Grem et al., 1993; de Gramont et al., 2000). However, the molecular mechanism(s) that cause the difference in the effect has not been made clear. We previously determined that oxaliplatin but not cisplatin was transported by OCT3 (Yonezawa et al., 2006; Yokoo et al., 2007). Therefore, we hypothesized that the level of hOCT3 in cancerous tissues contributed to the superior anticancer effect of oxaliplatin. In the present study, the level of hOCT3 mRNA was significantly higher in cancerous colon than in normal colon tissues derived from Japanese patients (Fig. 1A). In addition, this tendency was reproduced in Caucasians using a cancer profiling array (Fig. 7, A and B). These findings indicated that the level of hOCT3 mRNA was heightened by colorectal cancerous transformation independent of ethnicity.

In human colorectal cancer-derived cell lines, hOCT3 mRNA expression was correlated with the release of LDH and accumulation of platinum induced by the treatment with oxaliplatin (Fig. 6, A and B). These results suggested that hOCT3 expression is a candidate marker for the efficacy of oxaliplatin treatment. Moreover, the release of LDH and accumulation of platinum caused by the incubation with cisplatin was independent of the hOCT3 mRNA level (Fig. 6D). This result was consistent with the report that cisplatin was not transported by hOCT3 (Yonezawa et al., 2006). Therefore, hOCT3 expression is suggested to be closely associated with the anticancer activity of oxaliplatin but not that of cisplatin.

Cisplatin plays an essential role in chemotherapy against solid tumors of the prostate, bladder, lung, testis, liver, and brain (Ho et al., 2003). However, the effect of cisplatin on colorectal cancer is weak. Loehrer et al. (1988) and Grem et al. (1993) reported rates of response of colorectal cancer to cisplatin-based chemotherapy of 22 and 19%, respectively. On the other hand, for oxaliplatin-based chemotherapy, de Gramont et al. (2000) reported that the response rate was 50%. The differences in molecular mechanisms whereby cisplatin has a weak effect but oxaliplatin has a strong effect on colorectal cancer have been unclear. The anticancer activity and resistance to platinum agents have been considered to be related to the DNA repair pathway, nucleotide excision repair, base excision repair, mismatch repair, and double-strand break repair, or the substrate specificity of copper transporters, CTR1, ATP7A, and ATP7B (Kelland, 2007). However, recently, we and others reported the contribution of organic cation transporters in the cellular transport of platinum agents (Ciarimboli et al., 2005; Yonezawa et al., 2005, 2006; Zhang et al., 2006; Yokoo et al., 2007; Kitada et al., 2008). Zhang et al. (2006) reported that the effect of oxaliplatin against colon cancer was related to the expression of hOCT1 and hOCT2. Kitada et al. (2008) reported that the levels of ATP7A and hOCT1 mRNA affect the sensitivity to oxaliplatin. However, we reported that oxaliplatin was transported by both human and

TABLE 1

Platinum accumulation in colorectal cancer-derived cell lines (2 min)

Colorectal cancer-derived cell lines were treated with medium containing 100, 500, or 1000 μM oxaliplatin for 2 min. After being washed, these cells were solubilized in 0.5 N NaOH, and the amount of platinum was determined by ICP-MS. Each value represents the mean ± S.E. for four wells.

Cell Lines	Platinum Accumulation		
	100 μM	500 μM	1000 μM
	ng/mg protein/2 min		
T84	0.82 ± 0.03	5.12 ± 0.06	9.77 ± 0.46
SW480	0.48 ± 0.01	2.27 ± 0.02	4.19 ± 0.04
HCT116	0.46 ± 0.03	2.72 ± 0.08	5.23 ± 0.26
HT29	0.64 ± 0.01	3.55 ± 0.05	7.85 ± 0.19
SW837	1.07 ± 0.02	5.77 ± 0.10	14.3 ± 1.13
Lovo	0.61 ± 0.01	3.59 ± 0.07	7.27 ± 0.10

TABLE 2

Platinum accumulation in colorectal cancer-derived cell lines (1 h)

Colorectal cancer-derived cell lines were treated with medium containing 100, 500, or 1000 μM oxaliplatin for 1 h. After being washed, these cells were solubilized in 0.5 N NaOH, and the amount of platinum was determined by ICP-MS. Each value represents the mean ± S.E. for four wells.

Cell Lines	Platinum Accumulatioo		
	100 μM	500 μM	1000 μM
	ng/mg protein/hr		
T84	14.0 ± 0.3	70.5 ± 1.2	160.2 ± 3.9
SW480	4.9 ± 0.1	25.0 ± 0.5	64.0 ± 1.4
HCT116	6.0 ± 0.2	32.3 ± 0.6	79.2 ± 2.8
HT29	8.7 ± 0.1	47.8 ± 0.1	123 ± 2.6
SW837	16.7 ± 0.4	91.6 ± 2.3	222 ± 3.8
Lovo	9.6 ± 0.0	52.4 ± 1.2	126 ± 2.1

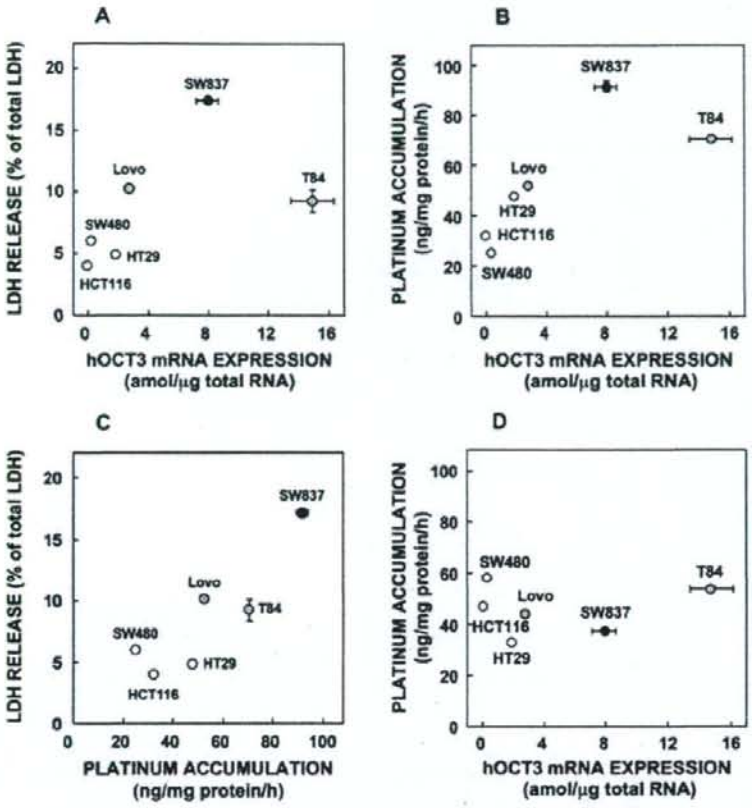

FIG. 6. Relation among hOCT3 mRNA expression, LDH release, and platinum accumulation. The data on mRNA expression are from Fig. 2, and the data on the release of LDH and accumulation of platinum are from Fig. 4B and Table 2, respectively. A, hOCT3 mRNA expression versus LDH release on treatment with 500 μM oxaliplatin. B, hOCT3 mRNA expression versus platinum accumulation on treatment with 500 μM oxaliplatin. C, platinum accumulation versus LDH release on treatment with 500 μM oxaliplatin. D, hOCT3 mRNA expression versus platinum accumulation on treatment with 500 μM cisplatin.

rat OCT2 and OCT3, but not by OCT1 (Yonezawa et al., 2006; Yokoo et al., 2007). In the present study, only hOCT3 mRNA was found in the six cell lines derived from colorectal cancers, and the cytotoxicity of oxaliplatin was associated with the expression level. Based on these findings and the present results, at least in colorectal cancer, OCT3 is thought to be important for sensitivity to oxaliplatin.

In the six colorectal cancer-derived cell lines, hOCT3 mRNA levels were markedly higher than hOCT1, hOCT2, hMATE1, or hMATE2-K mRNA levels (Fig. 2). Previously, we reported that oxaliplatin was also transported by hOCT2 (Yonezawa et al., 2006). However, in these cell lines, the expression of hOCT2 mRNA was little detected by real-time PCR (Fig. 2). Therefore, the contribution of hOCT2 to the anticancer effect of oxaliplatin was suggested to be small. The transport activity of hOCT3 in these cells was confirmed by using [^{3}H]MPP, a typical substrate of OCT3 (Fig. 3). Okuda et al. (2000) reported that the cytotoxicity of cisplatin differed at low and high doses, that is, 30 and 1000 μM cisplatin induced apoptosis and necrosis, respectively. In the present study, we used two indexes of cytotoxicity, LDH release and caspase 3/7 activity, as indicators of necrosis and apoptosis, respectively. Both LDH release and caspase activity showed a similar tendency; that is, values were high in cell lines expressing high levels of hOCT3 mRNA (Figs. 2 and 4, B and C). From these results, the hOCT3-mediated cellular accumulation of oxaliplatin might be a trigger for the subsequent cytotoxic effects.

Although the cytotoxicity of oxaliplatin in T84 cells was lower than expected, given the expression level of hOCT3 (Fig. 6A), the LDH release in these cells correlated quite well with the platinum accumulation (Fig. 6C). These results suggest some mechanisms including an unknown oxaliplatin efflux transporter to reduce the intracellular platinum concentration in T84 cells compared with that in SW837 cells.

We had reported that the nephrotoxicity caused by treatment with platinum agents was closely associated with their renal accumulation, which is determined by the substrate specificity of the OCT and MATE families (Yonezawa et al., 2005, 2006; Yokoo et al., 2007). There had also been a report that the uptake of imatinib, a tyrosine kinase inhibitor effective in the treatment of chronic myeloid leukemia, was mediated by hOCT1 (Thomas et al., 2004). Recently, two groups showed that hOCT1 was a determinant of outcome in imatinib-treated chronic myeloid leukemia (White et al., 2007; Wang et al., 2008). Patients with a high level of hOCT1 had a greater probability of achieving a cytogenetic response and superior progression-free and overall survival (Wang et al., 2008). These reports showed the participation of hOCT1 in the clinical effects of imatinib. Therefore, the results of this study, that the cytotoxicity of oxaliplatin depended on hOCT3 expression, may be expanded to include effectiveness in clinical cases.

OCT3 is widely distributed in many tissues (Kekuda et al., 1998), but its function has been examined mainly in the brain (Wu et al.,

DRUG METABOLISM AND DISPOSITION DMD aspet

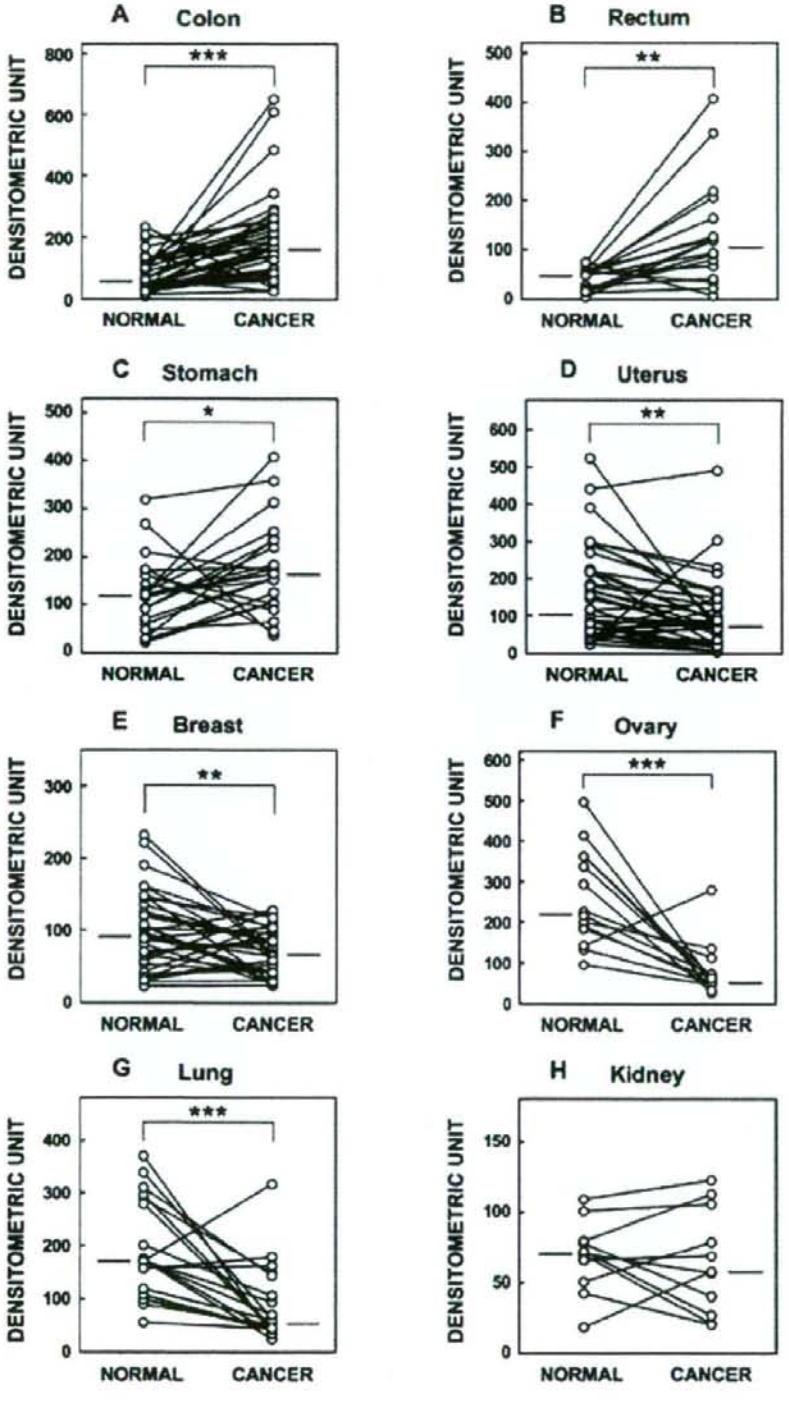

FIG. 7. The differences in hOCT3 expression between normal and cancerous tissues. The differences in hOCT3 expression between normal and cancerous tissue were examined by dot blotting. The density of each dot was quantified using ImageJ 1.38x. Figures represent the colon (A, n = 39), rectum (B, n = 18), stomach (C, n = 23), uterus (D, n = 42), breast (E, n = 35), ovary (F, n = 14), lung (G, n = 20), and kidney (H, n = 11). The bars represent median values.

1998; Gasser et al., 2006). The results of this study suggested a new role for OCT3, as a determinant of the sensitivity of treatment with oxaliplatin against colorectal cancer. At present, oxaliplatin is used for colorectal cancer as a key drug of FOLFOX regimens (de Gramont et al., 2000). Other combinations including oxaliplatin for colorectal cancer or other cancers have been used in clinical trials (Goldberg et al., 2004; Zhu et al., 2006). The level of hOCT3 in cancerous tissue was significantly higher in colon, rectum, and stomach (Fig. 7, A–C). Conversely, the level was significantly lower in uterus, breast, ovary, and lung (Fig. 7, D–G). These changes in hOCT3 expression might contribute to the sensitivity and selectivity of oxaliplatin-based chemotherapy. Recently, there were several reports that oxaliplatin was effective against gastric cancer in phase II trials (Lordick et al., 2005; Park et al., 2006; Kim et al., 2008). Considering the present results, there is a possibility that the increase of hOCT3 expression in cancerous tissue affects the results of clinical trials. Therefore, taking a positive attitude to use of oxaliplatin-based chemotherapy for other cancers that express high levels of hOCT3 compared with normal tissue may lead to good clinical results.

In the present study, we clearly found selective induction of hOCT3 mRNA expression in colon cancer and colorectal cancer-derived cell lines. The cytotoxicity and accumulation of platinum caused by the treatment with oxaliplatin but not cisplatin depended on the expression of hOCT3 mRNA. In conclusion, the uptake of oxaliplatin into the cancer cells via hOCT3 was suggested to be an important mechanism for its cytotoxicity, and the expression of hOCT3 in cancers may became a marker for including oxaliplatin in cancer chemotherapy.

References

André T, Boni C, Mounedji-Boudiaf L, Navarro M, Tabernero J, Hickish T, Topham C, Zaninelli M, Clingan P, Bridgewater J, Tabah-Fisch I, and de Gramont A (2004) Oxaliplatin, fluorouracil, and leucovorin as adjuvant treatment for colon cancer. *N Engl J Med* **350:**2343–2351.

Ciarimboli G, Ludwig T, Lang D, Pavenstädt H, Koepsell H, Piechota HJ, Haier J, Jaehde U, Zisowsky J, and Schlatter E (2005) Cisplatin nephrotoxicity is critically mediated via the human organic cation transporter 2. *Am J Pathol* **167:**1477–1484.

de Gramont A, Figer A, Seymour M, Homerin M, Hmissi A, Cassidy J, Boni C, Cortes-Funes H, Cervantes A, Freyer G, et al. (2000) Leucovorin and fluorouracil with or without oxaliplatin as first-line treatment in advanced colorectal cancer. *J Clin Oncol* **18:**2938–2947.

Fuertes MA, Alonso C, and Pérez JM (2003) Biochemical modulation of Cisplatin mechanisms of action: enhancement of antitumor activity and circumvention of drug resistance. *Chem Rev* **103:**645–662.

Gasser PJ, Lowry CA, and Orchinik M (2006) Corticosterone-sensitive monoamine transport in the rat dorsomedial hypothalamus: potential role for organic cation transporter 3 in stress-induced modulation of monoaminergic neurotransmission. *J Neurosci* **26:**8758–8766.

Goldberg RM, Sargent DJ, Morton RF, Fuchs CS, Ramanathan RK, Williamson SK, Findlay BP, Pitot HC, and Alberts SR (2004) A randomized controlled trial of fluorouracil plus leucovorin, irinotecan, and oxaliplatin combinations in patients with previously untreated metastatic colorectal cancer. *J Clin Oncol* **22:**23–30.

Grem JL, McAtee N, Balis F, Murphy R, Venzon D, Kramer B, Goldspiel B, Begley M, and Allegra CJ (1993) A phase II study of continuous infusion 5-fluorouracil and leucovorin with weekly cisplatin in metastatic colorectal carcinoma. *Cancer* **72:**663–668.

Ho YP, Au-Yeung SC, and To KK (2003) Platinum-based anticancer agents: innovative design strategies and biological perspectives. *Med Res Rev* **23:**633–655.

Inui K, Masuda S, and Saito H (2000) Cellular and molecular aspects of drug transport in the kidney. *Kidney Int* **58:**944–958.

Kekuda R, Prasad PD, Wu X, Wang H, Fei YJ, Leibach FH, and Ganapathy V (1998) Cloning and functional characterization of a potential-sensitive, polyspecific organic cation transporter (OCT3) most abundantly expressed in placenta. *J Biol Chem* **273:**15971–15979.

Kelland L (2007) The resurgence of platinum-based cancer chemotherapy. *Nat Rev Cancer* **7:**573–584.

Kim JG, Sohn SK, Chae YS, Song HS, Kwon KY, Do YR, Kim MK, Lee KH, Hyun MS, Ryoo HM, et al. (2008) Multicenter phase II study of docetaxel plus oxaliplatin combination chemotherapy in patients with advanced gastric cancer: Daegu Gyeongbuk Oncology Group. *Br J Cancer* **98:**542–546.

Kitada N, Takara K, Minegaki T, Itoh C, Tsujimoto M, Sakaeda T, and Yokoyama T (2008) Factors affecting sensitivity to antitumor platinum derivatives of human colorectal tumor cell lines. *Cancer Chemother Pharmacol* **62:**577–584.

Loehrer PJ Sr, Turner S, Kubilis P, Hui S, Correa J, Ansari R, Stephens D, Woodburn R, and Meyer S (1988) A prospective randomized trial of fluorouracil versus fluorouracil plus cisplatin in the treatment of metastatic colorectal cancer: a Hoosier Oncology Group trial. *J Clin Oncol* **6:**642–648.

Lordick F, Lorenzen S, Stollfuss J, Vehling-Kaiser U, Kullmann F, Hentrich M, Zumschlinge R, Dietzfelbinger H, Thoeditmann J, Hennig M, et al. (2005) Phase II study of weekly oxaliplatin plus infusional fluorouracil and folinic acid (FUFOX regimen) as first-line treatment in metastatic gastric cancer. *Br J Cancer* **93:**190–194.

Masuda S, Terada T, Yonezawa A, Tanihara Y, Kishimoto K, Katsura T, Ogawa O, and Inui K (2006) Identification and functional characterization of a new human kidney-specific H^+/organic cation antiporter, kidney-specific multidrug and toxin extrusion 2. *J Am Soc Nephrol* **17:**2127–2135.

Motohashi H, Sakurai Y, Saito H, Masuda S, Urakami Y, Goto M, Fukatsu A, Ogawa O, and Inui K (2002) Gene expression levels and immunolocalization of organic ion transporters in the human kidney. *J Am Soc Nephrol* **13:**866–874.

Okuda M, Masaki K, Fukatsu S, Hashimoto Y, and Inui K (2000) Role of apoptosis in cisplatin-induced toxicity in the renal epithelial cell line LLC-PK1: implication of the functions of apical membranes. *Biochem Pharmacol* **59:**195–201.

Park YH, Kim BS, Ryoo BY, and Yang SH (2006) A phase II study of capecitabine plus 3-weekly oxaliplatin as first-line therapy for patients with advanced gastric cancer. *Br J Cancer* **94:**959–963.

Raymond E, Faivre S, Chaney S, Woynarowski J, and Cvitkovic E (2002) Cellular and molecular pharmacology of oxaliplatin. *Mol Cancer Ther* **1:**227–235.

Terada T and Inui K (2008) Physiological and pharmacokinetic roles of H^+/organic cation antiporters (MATE/SLC47A). *Biochem Pharmacol* **75:**1689–1696.

Terada T, Shimada Y, Pan X, Kishimoto K, Sakurai T, Doi R, Onodera H, Katsura T, Imamura M, and Inui K (2005) Expression profiles of various transporters for oligopeptides, amino acids and organic ions along the human digestive tract. *Biochem Pharmacol* **70:**1756–1763.

Thomas J, Wang L, Clark RE, and Pirmohamed M (2004) Active transport of imatinib into and out of cells: implications for drug resistance. *Blood* **104:**3739–3745.

Urakami Y, Kimura N, Okuda M, and Inui K (2004) Creatinine transport by basolateral organic cation transporter hOCT2 in the human kidney. *Pharm Res* **21:**976–981.

Wang D and Lippard SJ (2005) Cellular processing of platinum anticancer drugs. *Nat Rev Drug Discov* **4:**307–320.

Wang L, Giannoudis A, Lane S, Williamson P, Pirmohamed M, and Clark RE (2008) Expression of the uptake drug transporter hOCT1 is an important clinical determinant of the response to imatinib in chronic myeloid leukemia. *Clin Pharmacol Ther* **83:**258–264.

White DL, Saunders VA, Dang P, Engler J, Venables A, Zrim S, Zannettino A, Lynch K, Manley PW, and Hughes T (2007) Most CML patients who have a suboptimal response to imatinib have low OCT-1 activity: higher doses of imatinib may overcome the negative impact of low OCT-1 activity. *Blood* **110:**4064–4072.

Wu X, Kekuda R, Huang W, Fei YJ, Leibach FH, Chen J, Conway SJ, and Ganapathy V (1998) Identity of the organic cation transporter OCT3 as the extraneuronal monoamine transporter (uptake2) and evidence for the expression of the transporter in the brain. *J Biol Chem* **273:**32776–32786.

Yokoo S, Yonezawa A, Masuda S, Fukatsu A, Katsura T, and Inui K (2007) Differential contribution of organic cation transporters, OCT2 and MATE1, in platinum agent-induced nephrotoxicity. *Biochem Pharmacol* **74:**477–487.

Yonezawa A, Masuda S, Nishihara K, Yano I, Katsura T, and Inui K (2005) Association between tubular toxicity of cisplatin and expression of organic cation transporter rOCT2 (Slc22a2) in the rat. *Biochem Pharmacol* **70:**1823–1831.

Yonezawa A, Masuda S, Yokoo S, Katsura T, and Inui K (2006) Cisplatin and oxaliplatin, but not carboplatin and nedaplatin, are substrates for human organic cation transporters (SLC22A1–3 and multidrug and toxin extrusion family). *J Pharmacol Exp Ther* **319:**879–886.

Zhang S, Lovejoy KS, Shima JE, Lagpacan LL, Shu Y, Lapuk A, Chen Y, Komori T, Gray JW, Chen X, et al. (2006) Organic cation transporters are determinants of oxaliplatin cytotoxicity. *Cancer Res* **66:**8847–8857.

Zhu AX, Blaszkowsky LS, Ryan DP, Clark JW, Muzikansky A, Horgan K, Sheehan S, Hale KE, Enzinger PC, Bhargava P, et al. (2006) Phase II study of gemcitabine and oxaliplatin in combination with bevacizumab in patients with advanced hepatocellular carcinoma. *J Clin Oncol* **24:**1898–1903.

Address correspondence to: Dr. Ken-ichi Inui, Department of Pharmacy, Kyoto University Hospital, Sakyo-ku, Kyoto 606-8507, Japan. E-mail: inui@kuhp.kyoto-u.ac.jp

Drug Metab. Pharmacokinet. 23 (6): 469–475 (2008).

Regular Article

Effect of Intestinal and Hepatic First-pass Extraction on the Pharmacokinetics of Everolimus in Rats

Akira YOKOMASU, Ikuko YANO, Eriko SATO,
Satohiro MASUDA, Toshiya KATSURA and Ken-ichi INUI*
Department of Pharmacy, Kyoto University Hospital, Faculty of Medicine, Kyoto University, Kyoto, Japan

Full text of this paper is available at http://www.jstage.jst.go.jp/browse/dmpk

Summary: The aim of this study was to quantitatively evaluate the effects of intestinal and hepatic extraction on the pharmacokinetics of everolimus in rats. Everolimus was administered intravenously, intraportally or intraintestinally in order to separately evaluate the intestinal and hepatic first-pass extraction. Cyclosporine or tacrolimus was administered into rat intestines, and after 10 min everolimus pharmacokinetics were evaluated. The blood concentrations of everolimus were measured by the high-performance liquid chromatography with tandem mass spectrometry. Total body clearance of everolimus was constant in the dosage from 0.2 to 1.0 mg/kg. The bioavailability after intraportal and intraintestinal administration were 48.0% and 21.2%, respectively. Concomitantly administered cyclosporine (5 mg/kg) , but not tacrolimus (1 mg/kg), significantly decreased the total body clearance of everolimus compared with the control, and also increased the bioavailabilty of everolimus after intraintestinal administration 1.75-fold. Cyclosporine significantly increased the area under the blood concentration-time curve of everolimus after the intraintestinal constant infusion 3-fold, and increased that after the intraportal constant infusion only 1.35-fold. In conclusion, the intestine as well as liver contributes to the first-pass extraction for everolimus in rats. Intestinally administered cyclosporine inhibited the intestinal extraction of everolimus more than its hepatic extraction.

Keywords: everolimus; first-pass effect; pharmacokinetics; cyclosporine; tacrolimus; interaction

Introduction

Everolimus is an immunosuppressive macrolide bearing a stable 2-hydroxyethyl chain substitution at position 40 on the sirolimus (rapamycin) structure. Both everolimus and sirolimus inhibit the mammalian target of rapamycin (mTOR) and suppress the activation of lymphocytes and cell proliferation.[1] Everolimus was developed in an attempt to improve the oral bioavailability of sirolimus,[2] and is used generally with a calcineurin inhibitor cyclosporine for renal or heart transplantations.[3–6] When everolimus is used together, synergistic pharmacological interactions are expected to potentiate the immunosuppressive effects of cyclosporine,[7] and the dose of cyclosporine can be reduced and various adverse effects, such as nephrotoxicity or neurotoxicity, caused by cyclosporine can be substantially decreased.[5,6]

Everolimus is absorbed rapidly, but has variable pharmacokinetics,[3,8] which is probably explained by different activities of drug efflux pump P-glycoprotein and of metabolism by the cytochrome P450 (CYP) 3A subfamily, as well as cyclosporine or tacrolimus.[9–11] Since higher blood concentrations of everolimus are related to the incidence of adverse effects such as hypertriglycemia, hypercholesterolemia and thrombocytopenia, blood concentration monitoring is required.[12] Therefore, pharmacokinetic interactions between everolimus and other drugs that inhibit the transport by P-glycoprotein and/or metabolism by CYP3A subfamily should be carefully considered to achieve safe therapies. It was reported that the blood concentration of everolimus was elevated with combination cyclosporine treatment in patients and rats,[2,7,13] probably due to inhibition of hepatic and/or intestinal metabolism of everolimus by cyclosporine. However, the quantitative contribution of intestinal and hepatic first-pass extraction of everolimus to its phar-

Received; February 29, 2008, Accepted; July 17, 2008
**To whom correspondence should be addressed:* Professor Ken-ichi INUI, Ph.D., *Department of Pharmacy, Kyoto University Hospital, Sakyo-ku, Kyoto 606-8507, Japan. Tel. +81-75-751-3577, Fax. +81-75-751-4207, Email: inui@kuhp.kyoto-u.ac.jp*
This work was supported in part by a Grant-in-aid for Scientific Research from the Ministry of Education, Culture, Sports, Science and Technology of Japan, and by the 21st Century COE Program 'Knowledge Information Infrastructure for Genome Science'.